GERMAN - MONGOLIAN INSTITUTE
FOR RESOURCES AND TECHNOLOGY

The present work was submitted to
the Faculty of Raw Materials and Environmental Engineering

OPTIMIZATION AND EVALUATION OF OPERATIONAL PERFORMANCE FOR MEMBRANE BIOREACTOR (MBR)

Bachelor's Thesis

By

UNDARMAA Dagdangonchig

Study program: Environmental Engineer

Student ID: B2200593

1st Supervisor/ Examiner: Dr. Ariuntuya Tserendorj

2nd Supervisor/ Examiner: Dr. Tamir Puntsag

Advisor: Ms. Dagiisuren Badamkhatan

Ulaanbaatar/Nalaikh

2026

GERMAN - MONGOLIAN INSTITUTE
FOR RESOURCES AND TECHNOLOGY

The present work was submitted to
the Faculty of Raw Materials and Environmental Engineering

OPTIMIZATION AND EVALUATION OF OPERATIONAL PERFORMANCE FOR MEMBRANE BIOREACTOR (MBR)

Bachelor's Thesis

By

UNDARMAA Dagdangonchig

Study program: Environmental Engineer

Student ID: B2200593

1st Supervisor/ Examiner: Dr. Ariuntuya Tserendorj

2nd Supervisor/ Examiner: Dr. Tamir Puntsag

Advisor: Ms. Dagiisuren Badamkhatan

Ulaanbaatar/Nalaikh

2026

Statutory Declaration

Dagdangonchig, Undarmaa	B2200593
Last Name, First Name	Student ID Number

I hereby affirm in lieu of an oath that I provided the submitted bachelor thesis

OPTIMIZATION AND EVALUATION OF OPERATIONAL PERFORMANCE FOR MEMBRANE BIOREACTOR (MBR)

I did not use any sources other than those stated. In case that the work is additionally submitted on a data medium, I declare that the written and the electronic form are completely identical. The work was not submitted in the same or similar form to any examination authority.

Ulaanbaatar, Mongolia 2026.05.29	D. Undarmaa
Place, Date	Signature

Abstract

This study evaluates the operational performance of a membrane bioreactor (MBR) system at the Khaanzaa Wastewater Treatment Plant (WWTP), operated under subcontract with the Oyu Tolgoi mining project in the Gobi region of Mongolia.

The assessment is based on laboratory experiments and statistical analysis of long-term operational data collected between 2024 and 2025. The results demonstrate that the MBR system achieves high treatment efficiency, with effective removal of chemical oxygen demand (COD) and ammonia under the studied conditions. A key finding is the strong inverse relationship between sludge wasting rate (Qw) and sludge retention time (SRT). Insufficient or irregular sludge wasting resulted in excessively high SRT, leading to aged biomass, increasing MLSS, poor sludge settleability, and unstable process performance. Statistical analysis further showed significant variability in MLSS and dissolved oxygen (DO), with frequent deviations from optimal ranges. Excessive DO levels contributed to unnecessary energy consumption, while low DO conditions risked reduced nitrification efficiency.

Membrane performance analysis demonstrated that permeability was strongly affected by fouling and operational conditions. Although periodic cleaning temporarily restored performance, rapid fouling recurrence indicated the need for more stable biological control. Based on these findings, optimization of sludge wasting and aeration control is recommended to maintain stable MLSS and SRT conditions. Maintaining an SRT of approximately 20 days and DO within the optimal range (1.5–2.5 mg/L) is essential for improving system stability, reducing fouling, and enhancing long-term MBR performance.

Acknowledgement

I would like to express my sincere gratitude to my supervisor, Dr. Ariuntuya Tserendorj, for her continuous guidance, valuable feedback, and support throughout the completion of this thesis. Her guidance helped me at every stage of the research and writing of this thesis, and her expertise greatly contributed to its successful completion.

I am also deeply thankful to my second supervisor, Dr. Tamir Puntsag, for her insightful comments, academic support, and valuable advice, which greatly enhanced the quality of this work. From the bottom of my heart, I would like to express my sincere appreciation to my advisor, Ms. Dagiisuren Badamkhatan, for her continuous support throughout my studies, as well as for providing essential data and research guidance. Her motivation and enthusiasm were truly inspiring.

My sincere appreciation is extended to Khaanzaa Wastewater Treatment Plant for providing operational data and for their warm welcome and introduction to the treatment facility, as well as to Oyu Tolgoi LLC for the opportunity to visit the site and gain valuable practical insights.

Finally, I would like to thank my family and friends for their support, encouragement, and understanding throughout my studies and the completion of this thesis.

Table of Content

Statutory Declaration i
Abstract ii
Acknowledgement iii
1. Introduction 1
1.1 Background 1
1.2 Objectives 2
2. State of Art 2
2.1 Wastewater Characteristics and Discharge Standards 2
2.2 Conventional Biological Wastewater Treatment 4
2.3 Biological Processes and Microbial Kinetics 5
2.3.1 Bacterial Growth Curve 5
2.3.2 Nitrification and Denitrification 6
2.3.3 Microbial Kinetics 7
2.3.4 Effect of Temperature on Microbial Kinetics 9
2.4 Membrane Bioreactor (MBR) Technology 10
2.4.1 MBR Principle 10
2.4.2 Types of Membranes 10
2.4.3 Membrane Fouling 13
2.4.4 Factors Affecting Fouling 15
2.4.5 Fouling Control Methods 15
2.5 Key Operational Parameters Affecting MBR Performance 16
2.5.1 Hydraulic Retention Time (HRT) 16
2.5.2 Sludge Retention Time (SRT) 16
2.5.3 Biomass mass balance 17
2.5.4 SVI – Sludge volume index 17
2.5.5 Mixed Liquor Suspended Solids (MLSS) 17
2.5.6 Dissolved Oxygen (DO) 18
3. Methodology 19
3.1 Khaanzaa Wastewater Treatment Plant 19
3.2 Data collection 22

3.3 Sample Collection 23
3.4 Parameters Measured 23
3.5 Statistical Analysis 27
4. Result and Discussion 28
4.1 Determination of Key Operational Parameters 28
4.1.1 Temperature-Corrected Kinetic Parameters 28
4.1.2 Calculation Based on Monod Kinetics 29
4.1.3 Biomass Mass balance 29
4.2 Laboratory Results 30
4.3 Sludge Characteristics and Observation 32
4.4 Operational Data Analysis and Performance Evaluation 34
5. Conclusion 43
Reference 44
Appendix A 45
Appendix B 47
Appendix C 50

List of Tables

Table 1. Mongolian wastewater discharge standards 3
Table 2. Design wastewater characteristics and mass loading rates 3
Table 3. Standard kinetic coefficients for BOD removal and nitrification at 20°C [1] 9
Table 4. General characteristics of membrane processes [1] 10
Table 5. Types of membrane fouling by responsible constituent [1] 14
Table 6. Typical MLSS concentrations [1] 17
Table 7. Typical operating condition for nitrification tank [1] 18
Table 8. ORP conditions for denitrification [1] 18
Table 9. Hydraulic retention time (HRT) and sludge retention time (SRT) 28
Table 10. Temperature correction of standard kinetic coefficients for COD oxidation 29
Table 11. Summary of theoretical kinetic parameters for COD and NH_4^+ removal 29
Table 12. BOD Measurement Over 5 days 30
Table 13. Total Nitrogen & Total Phosphate 30
Table 14. SO4 & Fe 30
Table 15. Chemical oxygen demand (COD) 31

Table 16. MLSS and MLVSS concentrations 31
Table 17. Wastewater characteristics of lab determination 2025 35
Table 18. Excess Aeration Energy Cost (2024–2025) [9] 38
Table 19. Descriptive Statistics of Sludge Flows (2024–2025) 39
Table 20. Statistical Summary of Membrane Permeability 41

List of Figures

Figure 1. Flowsheet of a conventional WWTP 4
Figure 2. Bacterial growth curve showing biomass and substrate (food) concentration 5
Figure 3. Graphical representation of the Monod model 7
Figure 4. Membrane module types 11
Figure 5. Membrane process schemes of pressurized and submerged membrane. 12
Figure 6. Submerged membrane with vacuum draw-off 12
Figure 7. Configuration of submerged membrane systems. 13
Figure 8. Hermia's membrane fouling mechanism 13
Figure 9. Waste activated sludge flow from an MBR 16
Figure 10. Flowsheet of Khaanzaa WWTP 19
Figure 11. Nitrification Tank 21
Figure 12. Denitrification tank 21
Figure 13. ORP sensor installation point in denitrification. 21
Figure 14. Membrane Bioreactor (MBR) tanks during operation and maintenance 21
Figure 15. Dewatered sludge with moisture content of 80-85% 21
Figure 16. Permeate sample from MBR effluent 21
Figure 17. Online multiparameter sensor 21
Figure 18. Screw press filter for sludge dewatering 22
Figure 19. Control panel 22
Figure 20. Apparatus Used for COD Determination 22
Figure 21. Apparatus Used for BOD Determination 24
Figure 22. Hach DR/870 Portable Colorimeter 26
Figure 23. Evaporation dishes after drying at 103–105°C (MLSS analysis). 26
Figure 24. Visual comparison of sludge samples from different treatment units 32
Figure 25. Comparison of Monthly Influent and Effluent Flow Rates 34

1. Introduction

1.1 Background

Wastewater treatment processes play a crucial role in protecting the aquatic ecosystem and human health. The Gobi region of Mongolia faces a severe water shortage crisis, where scarce freshwater resources are under increasing pressure from rapid industrial expansion, particularly large-scale mining operations. In this arid environment, water scarcity is further intensified by climate change, prolonged droughts, and the overextraction of groundwater, making the responsible management and treatment of wastewater not merely an environmental concern but a critical necessity for the region's survival. Efficient and reliable wastewater treatment technologies capable of meeting strict discharge standards are therefore essential to conserving and recycling water resources in the Gobi region.

Domestic wastewater treatment processes, such as activated sludge systems, have been widely used to remove organic matter and nutrients. However, these systems often struggle to achieve consistently high effluent quality and may require large land areas and secondary clarification units. In recent years, membrane-based technologies, particularly membrane bioreactor (MBR) systems, have emerged as an advanced alternative that combines biological treatment with membrane filtration to produce higher-quality effluent. MBR systems offer several advantages over conventional treatment processes, including higher biomass concentrations, improved effluent quality, reduced footprint, and better resistance to hydraulic and organic loading variations. Despite these advantages, MBR systems are associated with significant operational challenges, the most critical of which is membrane fouling. Fouling results in increased transmembrane pressure (TMP), reduced permeate flux, and higher energy and maintenance costs, ultimately affecting system performance and operational efficiency [1].

The “Khaanzaa” LLC, in charge of the domestic wastewater treatment plant, subcontracted with the Oyu Tolgoi mining project, which uses an MBR system as the final treatment stage for domestic wastewater [2]. The plant operates under variable loading conditions and environmental constraints, making it a suitable case study for evaluating the operational performance of MBR systems. The system is designed to treat approximately 2000 m^3/day of wastewater, reflecting typical conditions of mining-related wastewater treatment facilities. Given the operational challenges caused by membrane fouling and energy consumption,

optimizing the MBR system performance is essential to ensure stable operation, reduce costs, and improve sustainability [2]. Operational parameters such as hydraulic retention time (HRT), sludge retention time (SRT), mixed liquor suspended solids (MLSS), aeration rate, and membrane flux play a critical role in determining system performance.

1.2 Objectives

This study aims to evaluate and optimize the operational performance of an MBR system using real operational data. The study focuses on the analysis of key performance indicators, including biochemical oxygen demand (BOD), chemical oxygen demand (COD), total suspended solids (TSS), permeate flux normalized by transmembrane pressure (TMP), and energy consumption. The specific objectives of this study are:

- To test or determine parameters for each treatment processes
- To collect data on the operational treatment performance based on key indicators
- To compare and assess the data using statistical analysis results.
- To investigate relationships between operational parameters and performance
- To propose optimized operational conditions to enhance system efficiency and reduce fouling

This research provides practical insights into the optimization of MBR systems under real operating conditions and contributes to improving wastewater treatment performance in mining environments in Mongolia.

2. State of Art

2.1 Wastewater Characteristics and Discharge Standards

Domestic wastewater is primarily composed of organic matter, suspended solids, nutrients, and various dissolved substances generated from human activities. The key pollution indicators typically include biochemical oxygen demand (BOD), chemical oxygen demand (COD), total suspended solids (TSS), ammonia (NH_4^+), total nitrogen (TN), and total phosphorus (TP). These parameters are widely used to evaluate wastewater strength and treatment efficiency. In Mongolia, wastewater discharge is regulated by national standards such as MNS 6561:2024 and MNS 4943:2024, which define the allowable limits for influent to sewer networks and treated effluent discharged into the environment [3]. These standard limits are summarized in Table 1.

Table 1. Mongolian wastewater discharge standards [3]

№	Quality induicator	Unit	MNS6561:2024	MNS4943:2015
1	BOD at 5 days	mg O2 /dm3	400	20
2	COD	mg O2 /dm3	800	50
3	Total Nitrogen	mg N/dm3	40	15
4	Total phosphorus	mg P/dm3	5	1.5
5	Ammonium, NH4	mg/dm3	20	-
6	Total iron	mg/dm3	3	1
7	Sulfate	mg/dm3	700	-

Domestic wastewater generation is assumed to be equal to domestic water consumption. According to the Mongolian construction norms and standards [8], the average daily water consumption per person is assumed to be 150 L/person·day. Based on typical design values, the average pollutant generation per capita is approximately 60 g BOD/person·day and 130 g COD/person·day. Assuming a design water consumption of 150 L/person·day, the corresponding influent concentrations are estimated to be around 400 mg/L for BOD and 867 mg/L for COD. Similarly, the concentrations of other key parameters are estimated as 467 mg/L for TSS, 67 mg/L for ammonia (NH_3), 100 mg/L for total nitrogen (TN), and 17 mg/L for total phosphorus (TP), as summarized in Table 2.

Table 2. Design wastewater characteristics and mass loading rates

Parameter	Unit	Per capita load (g/EP/day) [1]	Influent concentration (mg/l)
BOD	mg/L	60	400
COD	mg/L	130	867
TSS	mg/L	70	467
NH_3 (Ammonia)	mg/L	10	67
TN (Total Nitrogen)	mg/L	15	100
TP (Total Phosphorus)	mg/L	2.5	17

2.2 Conventional Biological Wastewater Treatment

Conventional wastewater treatment consists of a series of sequential stages designed to progressively remove physical, chemical, and biological contaminants from wastewater. As illustrated in Figure 1, a typical conventional treatment plant comprises preliminary and primary treatment, secondary biological treatment, and sludge treatment. In the preliminary and primary treatment stage, wastewater passes through screens to remove large solids, followed by grit removal to eliminate heavy inorganic particles, and primary clarification to remove settleable suspended solids [1]. In the secondary treatment stage, the primary effluent enters a biological reactor where microorganisms degrade dissolved organic matter. The mixed liquor is then separated in a secondary clarifier, with settled sludge recycled back to the biological reactor to maintain biomass concentration. The treated effluent is disinfected before discharge. Residual sludge from both primary and secondary clarifiers undergoes sludge treatment through gravity thickening, anaerobic digestion, and centrifugation, producing biosolids suitable for land application [4]. Despite its widespread use, conventional treatment has notable limitations. The reliance on gravity-based secondary clarification makes the process vulnerable to sludge bulking and inconsistent effluent quality. Large land areas are required, and effluent quality may be insufficient to meet strict effluent standards without additional tertiary treatment. These limitations have driven the adoption of membrane bioreactor (MBR) technology, which replaces the secondary clarifier with membrane filtration, as discussed in Section 2.4 [4].

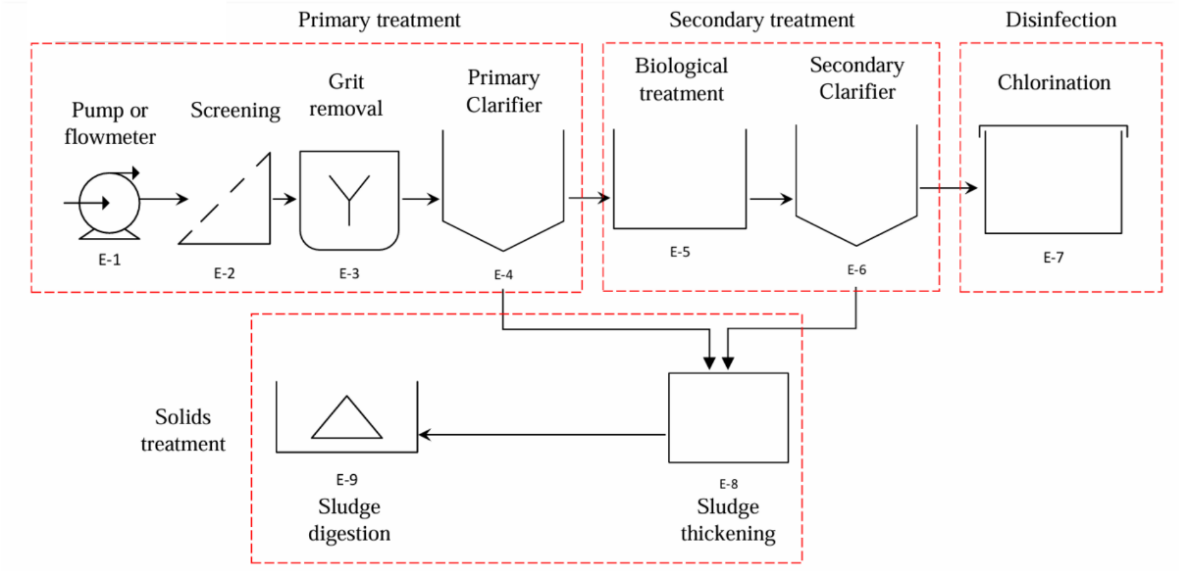


Figure 1. Flowsheet of a conventional WWTP

2.3 Biological Processes and Microbial Kinetics

2.3.1 Bacterial Growth Curve

The bacterial growth curve exhibits four distinct phases, as illustrated in Figure 2. In the lag phase, bacteria adjust to the new environment and synthesize the enzymes necessary to degrade the surrounding substrate. The duration of this phase depends on the biodegradability of the substrate. In the exponential (log) phase, substrate is abundant and the bacterial population doubles at regular intervals under optimal growth conditions, resulting in rapid biomass accumulation and a steep decline in substrate concentration. As substrate concentration decreases, the stationary phase is reached, where the growth rate equals the death rate and biomass concentration peaks at a dynamic equilibrium. Finally, in the endogenous decay (death) phase, substrate is completely exhausted and biomass concentration begins to decline as cell death and lysis occur [4].

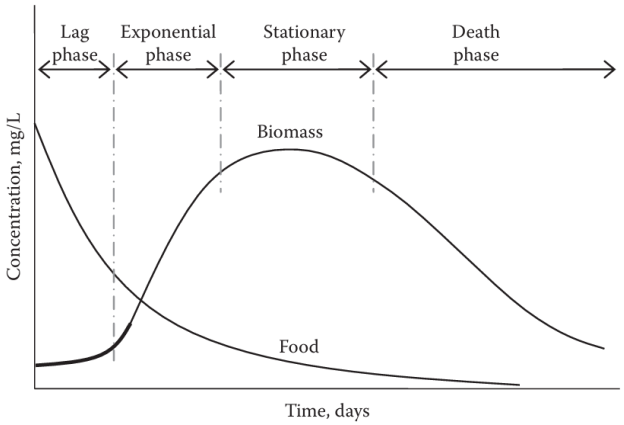


Figure 2. Bacterial growth curve showing biomass and substrate (food) concentration over time

Bacterial cells can be classified into two broad groups according to their carbon and energy source. Heterotrophic bacteria use organic compounds as both their carbon and energy source and represent the majority of bacteria in wastewater treatment systems, being responsible for organic matter (COD/BOD) removal. Autotrophic bacteria use inorganic compounds such as CO_2 and HCO_3^- as their carbon source and obtain energy from inorganic oxidation reactions. Of particular significance in wastewater treatment are chemoautotrophic nitrifying bacteria which obtain energy from the oxidation of ammonia and are responsible for biological nitrogen removal through nitrification [4].

Bacteria are further classified based on their oxygen requirements. Aerobic bacteria require oxygen for growth and survival, anaerobic bacteria grow only in the absence of oxygen, and

facultative bacteria can grow under both aerobic and anoxic conditions. Denitrifying bacteria are facultative anaerobes that use nitrate (NO_3^-) as an electron acceptor under anoxic conditions, converting it to nitrogen gas (N_2) [4].

2.3.2 Nitrification and Denitrification

Biological nitrogen removal (BNR) is a fundamental requirement in modern wastewater treatment, as elevated concentrations of ammonia and nitrate in receiving water bodies can lead to eutrophication, oxygen depletion, and toxicity to aquatic organisms. BNR involves two sequential microbially mediated processes: nitrification and denitrification [1].

Nitrification is an aerobic, two-stage biological process in which ammonia nitrogen (NH_4^+) is sequentially oxidized to nitrite (NO_2^-) and subsequently to nitrate (NO_3^-). This process is carried out by two distinct groups of chemoautotrophic bacteria, Nitrosomonas and Nitrobacter, which utilize CO_2 as a carbon source and obtain energy from inorganic oxidation reactions [1].

Nitrosomonas are responsible for the oxidation of ammonia to nitrite (NO_2^-) and play a key role as rate-limiting organisms in the nitrification process. They are highly sensitive to environmental conditions such as temperature, pH, and dissolved oxygen.

$$NH_4^+ + O_2 \rightarrow NO_2^- + H_2O + \text{Energy} \quad (2.1)$$

Nitrite is oxidized to nitrate (NO_3^-) by Nitrobacter, which are aerobic bacteria responsible for the second step of nitrification. This process generally proceeds rapidly under aerobic conditions and is not typically the rate-limiting step under normal operating conditions.

$$NO_2^- + O_2 \rightarrow NO_3^- + \text{Energy} \quad (2.2)$$

Overall nitrification reaction:

$$NH_4^+ + 2O_2 \rightarrow NO_3^- + 2H^+ + H_2O \quad (2.3)$$

As autotrophic organisms, nitrifying bacteria exhibit significantly lower growth rates compared to heterotrophic bacteria responsible for organic carbon removal. The maximum specific growth rate of *Nitrosomonas* is approximately 0.9 d^{-1} at 20°C, and the half-saturation constant for ammonia (K_s) is approximately 0.5 mg NH_4^+/L. Due to these slow growth kinetics, maintaining a sufficiently long sludge retention time (SRT ≥ 10–25 days) is essential to prevent washout of nitrifying organisms from the system [1].

Denitrification is the biological reduction of nitrate (NO_3^-) to nitrogen gas (N_2), which is released to the atmosphere, thereby completing the nitrogen cycle. This process is carried out by heterotrophic facultative anaerobic bacteria, including Alcaligenes, Pseudomonas, and Bacillus species under anoxic conditions, using nitrate as the terminal electron acceptor.

The reduction pathway proceeds through a sequence of intermediate reactions:

$$NO_3^- \rightarrow NO_2^- \rightarrow NO \rightarrow N_2O \rightarrow N_2 \text{ (gas released to atmosphere)} \quad (2.4)$$

The process requires an organic carbon source as an energy substrate for microbial activity. In conventional wastewater treatment, biodegradable COD present in the influent typically serves as the primary carbon source. It occurs under anoxic conditions (DO ≈ 0), where nitrate or nitrite replaces oxygen as the electron acceptor [4].

Using organic carbon as electron donor, the overall reaction can be expressed as:

$$NO_3^- + \text{Organic C} \rightarrow N_2 + CO_2 + H_2O \quad (2.5)$$

The corresponding electron acceptor reaction is:

$$NO_3^- + 5e^- + 6H^+ \rightarrow \tfrac{1}{2}N_2 + 3H_2O \quad (2.6)$$

2.3.3 Microbial Kinetics

Microbial Growth Rate

The Monod model is one of the earliest and most widely adopted frameworks for scribing microbial growth in biological reactors. The model assumes that substrate utilization and biomass growth rates are controlled by enzymatic reactions involving the limiting substrate [4]. The Monod equation for microbial growth is expressed as:

$$\mu = \mu_{max} \frac{S}{K_S + S} \quad (2.7)$$

where μ is the specific growth rate (d^{-1}), μ_{max} is the maximum specific growth rate (d^{-1}), S is the substrate concentration (mg/L) and K_S is the half-saturation constant.

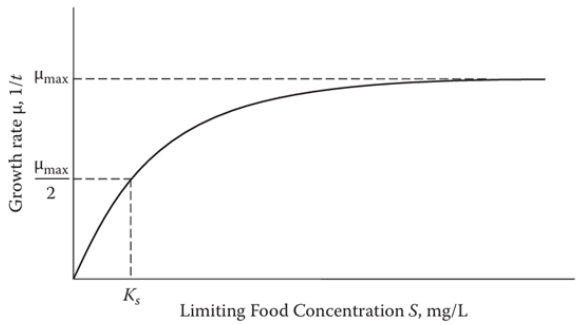


Figure 3. Graphical representation of the Monod model

As illustrated in Figure 3, the biomass growth rate is a hyperbolic function of substrate concentration. When substrate is abundant (S >> Ks), the growth rate approaches its maximum value (μ ≈ μmax). Under substrate-limiting conditions (S << Ks), the growth rate becomes proportional to substrate concentration. At S = Ks, the growth rate is equal to half of μmax. In practice, activated sludge and MBR systems are typically operated under substrate-limited conditions to achieve low effluent substrate concentrations through appropriate control of sludge retention time (SRT) [4].

Biomass yield is an additional key parameter that describes the amount of biomass produced per unit of substrate consumed:

$$Y = \frac{mg\ biomass\ produced}{mg\ substrate\ utilized} \tag{2.8}$$

Biomass concentration in the reactor is measured as total suspended solids (TSS) or volatile suspended solids (VSS). Typical yield values are 0.4–0.8 g VSS/g BOD for aerobic conditions and 0.08–0.2 g VSS/g BOD for anaerobic conditions [1].

The Monod model provides a theoretical framework from which key design equations can be developed to relate substrate concentration, biomass concentration, and operational parameters such as sludge retention time (SRT). These equations are fundamental tools for the analysis and design of biological treatment systems, including activated sludge and MBR processes [4].

Effluent Substrate Concentration

$$S = \frac{Ks(1 + k_d \times SRT)}{SRT \times (Y \times\ \mu max - k_d) - 1} \tag{2.9}$$

Biomass X

$$X = \frac{SRT \times Y \times (S_0 - S)}{\tau(1 + k_d \times SRT)} \tag{2.10}$$

Net Biomass Yield

$$Y_{net} = \frac{Y}{1 + k_d \times SRT} \tag{2.11}$$

Net specific growth rate

$$\mu_{net} = \mu - k_d \tag{2.12}$$

Verification via 1/SRT Relationship

$$\frac{1}{SRT} = Y \times U - K_d \tag{2.13}$$

where U is the specific substrate utilisation rate (d^{-1}):

$$U = \frac{S_0 - S}{\tau \cdot X} \tag{2.14}$$

F/M ratio

$$\frac{F}{M} = \frac{S_0 - S}{\tau \times X} \tag{2.15}$$

The standard kinetic coefficients for biological treatment processes at 20°C are summarized in Table 3.

Table 3. Standard kinetic coefficients for BOD removal and nitrification at 20°C [1]

	Kinetic Coefficient	COD Oxidation	NH_4^+ Oxidation	NO_2^- Oxidation
$\boldsymbol{\mu_{max}}$	Maximum specific growth rate, T^{-1} (g VSS/g VSS d)	6.0	0.90	1.0
$\boldsymbol{K_S}$	Half velocity constant, ML^{-3} (mg/L)	8.0	0.50	0.20
$\boldsymbol{Y}$	Biomass yield, M of cell formed per M of substrate consumed (g VSS/g substrate oxidized)	0.45	0.15	0.05
$\boldsymbol{K_d}$	Endogenous decay coefficient, T^{-1} (mg VSS/mg VSS d)	0.12	0.17	0.17
$\boldsymbol{\theta}$	Values			
	μ_{max}	1.07	1.072	1.063
	K_S	1.04	1.029	1.029
	K_d	1.0	1.0	1.0

2.3.4 Effect of Temperature on Microbial Kinetics

The van't Hoff–Arrhenius model describes the effect of temperature on biochemical reaction rates in biological treatment systems. According to this model, the reaction rate coefficient increases exponentially with temperature and can be expressed as a function of a reference value at 20°C and a temperature correction factor. This relationship is widely used to adjust kinetic parameters such as substrate utilization and microbial growth rates under varying temperature conditions [1].

$$K_T = K_{20} \times \theta^{T-20} \tag{2.16}$$

where K_T is the reaction rate coefficient at temperature T (°C), k_{20} is the reaction rate coefficient at 20°C, θ is the temperature activity coefficient (Arrhenius coefficient), and T is the operating temperature (°C).

The Arrhenius coefficient θ typically ranges from 1.02 to 1.25 depending on the process, with a commonly used value of θ = 1.047 for BOD removal.

2.4 Membrane Bioreactor (MBR) Technology

2.4.1 MBR Principle

A membrane bioreactor (MBR) is an advanced wastewater treatment technology that combines a biological reactor with membrane filtration. The biological reactor functions similarly to a conventional activated sludge process, where microorganisms degrade organic matter and nutrients. However, unlike conventional systems that rely on gravity-based secondary clarification, MBR systems use porous membranes with pore diameters of 0.05–0.1 μm to separate treated effluent from the activated sludge [5]. Due to the small pore size, the membrane effectively retains activated sludge flocs, free-living bacteria, and large viruses, producing a high-quality effluent. Compared to conventional activated sludge processes with gravity clarifiers, MBR systems offer several key advantages including much smaller area requirement (less than 50%) due to operation with a higher mixed liquor concentration and a lower disinfection does requirement due to the low turbidity effluent [1]. However, MBR systems are associated with higher energy costs, the need for future membrane replacement, and ongoing operational demands for membrane fouling control.

2.4.2 Types of Membranes

Membranes used in water and wastewater treatment are classified into five types based on pore size and separation mechanism, as summarized in Table 4.

Table 4. General characteristics of membrane processes [1]

Membrane process	Pore Size	Typical Operating Range (μm)	Separation Mechanism	Constituents Removed
Microfiltration (MF)	> 50 nm	0.07–2.0	Sieve	Suspended solids, bacteria, protozoa
Ultrafiltration (UF)	2–50 nm	0.008–0.2	Sieve	Colloids, proteins, viruses
Nanofiltration (NF)	< 2 nm	0.0009–0.01	Sieve + diffusion + exclusion	Divalent ions, small organics

Reverse Osmosis (RO)	< 2 nm (dense)	0.0001–0.002	Solution/diffusion + exclusion	Monovalent ions, all dissolved
Electrodialysis	—	0.0003–0.002	Ion exchange	Ionic species

In MBR systems, microfiltration (MF) and ultrafiltration (UF) membranes are most commonly applied, as they effectively remove suspended solids, bacteria, and colloidal matter while operating at relatively low transmembrane pressures.

Membrane modules are available in four physical configurations, as presented in Figure 4. (a) tubular, (b) hollow fiber, (c) spiral wound, and (d) plate and frame. Among these, hollow fiber modules are most widely used in MBR applications due to their high packing density, ease of backwashing, and suitability for submerged operation [1].

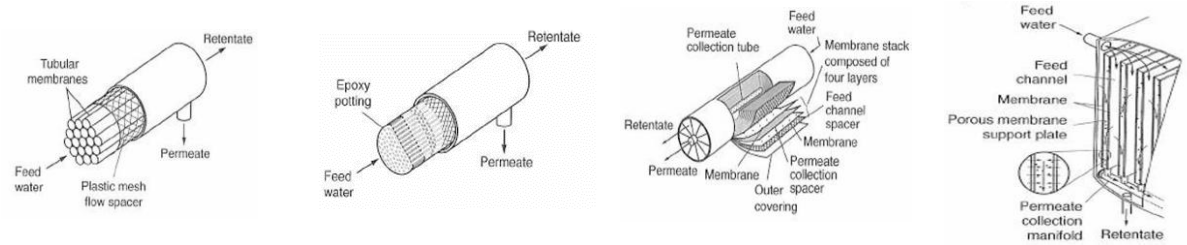


Figure 4. a). Tubular b). Hollow fiber c). Spiral wound d). Plate and frame

MBR systems operate in two configurations based on membrane placement (Figure 5). In the pressurized (sidestream) configuration, the membrane module is located outside the bioreactor and mixed liquor is pumped through it under pressure. In the submerged configuration, the membrane modules are installed directly inside the bioreactor or in a separate membrane tank immediately after the bioreactor, and permeate is extracted by a suction pump under slight vacuum. The submerged configuration is more energy-efficient and is the most widely adopted design in municipal wastewater treatment [1].

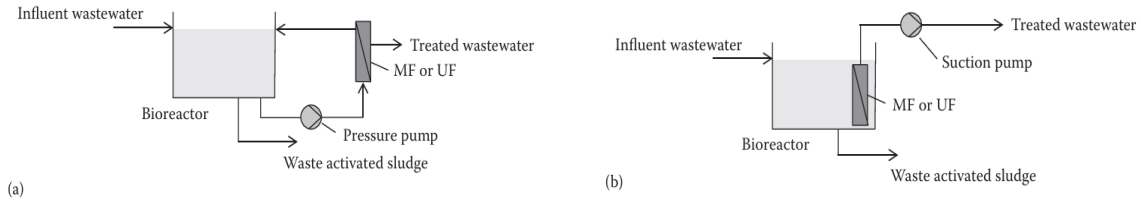


Figure 5. Configuration of submerged membrane systems

As illustrated in Figure 6, two submerged MBR configurations are commonly used. In configuration (e), permeate is extracted by a vacuum pump in a single direction, with air scouring providing fouling control at the membrane surface. In configuration (f), a backwash pump periodically reverses the permeate flow using treated water from the permeate tank to flush accumulated solids from the membrane surface, providing more effective fouling control [1].

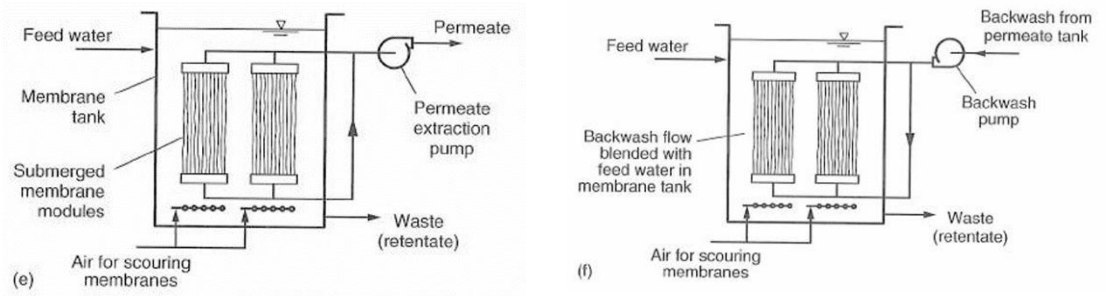


Figure 6. e). submerged membrane with vacuum draw-off and f). backwashing submerged system

In submerged MBR systems, membrane modules are assembled into cassettes, which are then installed as process trains within the membrane tank, as shown in Figure 7. Individual hollow fiber or flat sheet membrane modules are first grouped into a cassette unit, and multiple cassettes are combined to form a process train that fits within the bioreactor or membrane tank [5].

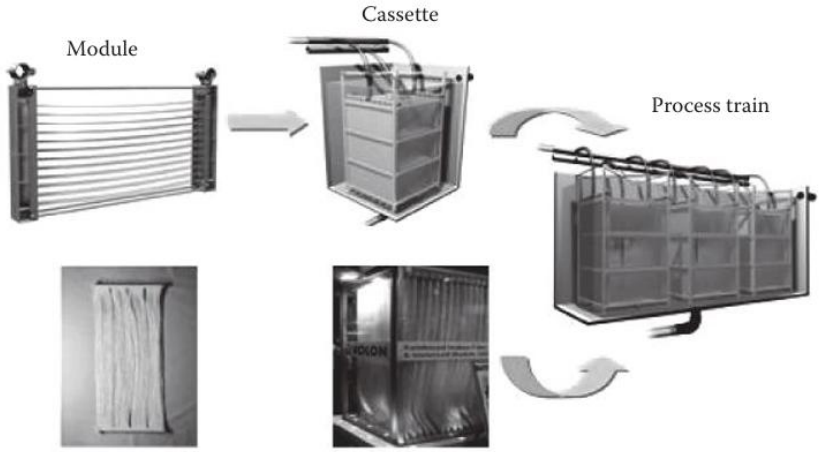


Figure 7. Configuration of submerged membrane systems

Membrane permeability is a key performance indicator defined as:

$$L_p = \frac{J}{\Delta P} \tag{2.17}$$

where L_p is the water permeability of the membrane, LMH/bar, J is the water flux of the membrane, LMH, L/m2 h, ΔP is the transmembrane pressure (TMP), bar. A decline in permeability over time is a direct indicator of membrane fouling [5].

2.4.3 Membrane Fouling

Membrane fouling is defined as the reduction or loss of membrane performance due to the deposition of particulate or dissolved substances on the membrane surface or within the membrane pore structure [5]. Fouling intensity in MBR systems can be expressed through two criteria: permeate flux and fouling resistance, calculated using the resistance-in-series (RIS) model:

$$J = \frac{\Delta P}{\eta * R} \tag{2.18}$$

$$R_t = R_m + R_C + R_a \tag{2.19}$$

where J is the permeation flux (LMH), ΔP is the TMP (bar), η is the viscosity of water (bar·s), R_t is the total resistance (m^{-1}), R_m is the membrane resistance, R_C is the cake layer resistance, and R_a is the adsorption resistance [5].

As illustrated in Figure 8, membrane fouling occurs through four distinct physical mechanisms [5]:

(a) Complete blocking — particles completely seal individual membrane pores
(b) Internal pore blocking — particles deposit inside the pore channels, narrowing the flow path
(c) Intermediate blocking — particles accumulate on the membrane surface, partially covering pore openings
(d) Cake formation — a layer of accumulated particles forms on the membrane surface, creating additional hydraulic resistance

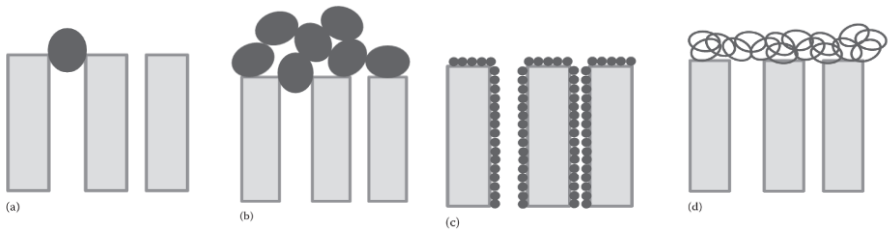


Figure 8. Hermia's membrane fouling mechanism: (a) complete blocking, (b) internal pore blocking, (c) intermediate blocking, and (d) cake formation.

Membrane fouling is traditionally classified into reversible and irreversible fouling based on the capability of flux recovery after cleaning [5] .Reversible (recoverable) fouling refers to fouling that can be restored by simple physical cleaning methods such as backwashing, pressure relaxation, and air scouring. Irrecoverable fouling originates from the consolidation of a gel layer at the interface between the membrane surface and the cake layer, as well as from strong adsorption of solutes to the pore walls, and can only be removed by chemical cleaning. Irreversible fouling represents permanent membrane deterioration that cannot be recovered by any means of cleaning. The relationship between these fouling types is expressed as [5]:

$$TF = RF + IF = REF + IRF + IF \quad (2.20)$$

where TF is the total fouling, RF is the reversible fouling, IF is the irreversible fouling, REF is the recoverable fouling and IRF is the irrecoverable fouling.

As membrane filtration progresses, TMP increases gradually. Periodic backflushing maintains TMP as low as possible during early operation. However, irreversible fouling, although relatively small at the initial stage, develops gradually over time and leads to permanent permeability loss.

Table 5. Types of membrane fouling by responsible constituent [1]

Type of Fouling	**Responsible Constituents**	**Control Method**
Particulate fouling	Colloids, emulsified oils, clays, metal oxides	Regular physical cleaning
Scaling	Calcium carbonate, calcium phosphate, barium sulfate	pH control, antiscalant addition
Organic fouling	NOM, humic acids, proteins, polysaccharides	Pretreatment, chemical cleaning SRT control, chlorination
Biological (Biofouling)	Bacteria, EPS, living/dead microorganisms	SRT control, chlorination

Membrane fouling can further be categorized according to the type of wastewater constituent responsible, as summarized in Table 5. Particulate fouling is caused by organic and inorganic colloids, emulsified oils, clays, and metal oxides, and can be reduced by regular physical cleaning. Scaling occurs when supersaturated salts such as calcium

carbonate and calcium phosphate precipitate on the membrane surface as their concentrations exceed solubility limits, and is controlled by pH adjustment and antiscalant addition. Organic fouling results from the accumulation of natural organic matter (NOM), humic acids, and proteins on the membrane surface, forming a stable fouling layer that reduces permeability. Biological fouling (biofouling) presents a particular challenge in MBR systems, elevated concentrations of organic matter and nutrients at the membrane surface promote microbial colonization, and as bacteria grow into the membrane pores and produce extracellular polymeric substances (EPS), permeability declines progressively [1].

2.4.4 Factors Affecting Fouling

Several operational and biological factors influence the rate and severity of membrane fouling in MBR systems. Higher MLSS concentrations increase the viscosity of the mixed liquor, reducing dissolved oxygen transfer and membrane permeability. Extracellular polymeric substances (EPS) and soluble microbial products (SMP) secreted by bacteria are major contributors to biofouling, as they adsorb onto the membrane surface and accelerate cake layer formation. Operating at SRT values below 10 days has been shown to increase EPS production and fouling tendency, while longer SRTs of 20–50 days result in better membrane performance [1]. Operating above the critical flux threshold causes a rapid and irreversible rise in TMP, making flux control a critical operational parameter.

2.4.5 Fouling Control Methods

Membrane fouling control strategies in MBR systems are broadly classified into two categories: direct membrane cleaning and fouling prevention [5]. Direct membrane cleaning involves methods applied after fouling has occurred, including chemical cleaning using acids, bases, ozone, NaOCl, and polyelectrolytes; physical methods such as coarse aeration, backwashing, and two-phase flow; and combined physical-chemical approaches such as chemically enhanced backwashing. Fouling prevention strategies aim to minimize fouling before it occurs through physical pretreatment of debris, hair, and grit; critical flux operation to avoid exceeding the threshold flux; biological control through adjustment of HRT, SRT, F/M ratio, DO, and MLSS and membrane/module development including antifouling membranes and shear-enhancing module designs. Emerging approaches include electrical methods such as in situ EC and DC induction, and biological-chemical strategies such as quorum quenching and nitric oxide application [5].

2.5 Key Operational Parameters Affecting MBR Performance

The performance of MBR systems is governed by a set of critical operational parameters that influence both biological treatment efficiency and membrane filtration performance. The key parameters monitored and evaluated in this study include hydraulic retention time (HRT), sludge retention time (SRT), mixed liquor suspended solids (MLSS), dissolved oxygen (DO), permeate flux, and transmembrane pressure (TMP).

2.5.1 Hydraulic Retention Time (HRT)

Hydraulic Retention Time (HRT) is a fundamental design parameter that describes the average time a unit volume of liquid remains within a biological reactor. It is defined by the ratio of the reactor volume to the volumetric flow rate of the influent:

$$\tau = V / Q \tag{2.21}$$

where τ is the hydraulic retention time (d), V is the reactor volume (m^3), and Q is the influent flow rate (m^3/d) [4].

2.5.2 Sludge Retention Time (SRT)

The Sludge Retention Time (SRT), also referred to as the mean cell residence time or sludge age, is defined as the ratio of the total mass of solids held within the biological system to the mass of solids wasted per day [1].

$$SRT = \frac{VX}{Q_w \times X_w + Q_e \times X_e} \tag{2.22}$$

where V is the reactor volume (m^3), X is the biomass concentration in the reactor (mg/L), Q_w is the waste sludge flow rate (m^3/day), X_w is the biomass concentration in the wasted sludge (mg/L), Q_e is the effluent flow rate (m^3/day), and X_e is the effluent total suspended solids (TSS) concentration (mg/L).

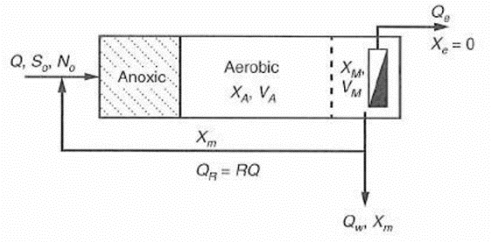


Figure 9. Waste activated sludge flow from an MBR

2.5.3 Biomass mass balance [1]

$$Q_{in} \times X_{in} + Q_r \times X_r = Q_{eff} \times X_{eff} + Q_w \times X_w \quad (2.23)$$

where Q_{in} is the influent flow rate (m³/day), X_{in} is the influent biomass concentration (mg/L), Q_r is the return activated sludge flow rate (m³/day), X_r is the biomass concentration in the return sludge (mg/L), Q_{eff} is the effluent flow rate (m³/day), X_{eff} is the biomass concentration in the effluent (mg/L), Q_w is the waste sludge flow rate (m³/day) and X_w is the biomass concentration in the waste sludge (mg/L).

2.5.4 SVI – Sludge volume index

The settleability of the activated sludge was assessed using the Sludge Volume Index (SVI), which represents the volume occupied by 1 g of settled sludge after 30 minutes of settling. SVI was calculated as [6]:

$$SVI = \frac{V \times 1000}{MLSS} \quad (2.24)$$

where SVI is the sludge volume index (mL/g), V is the volume of settled sludge (mL/L), and MLSS is the mixed liquor suspended solids (mg/L).

SVI values below 100 mL/g are considered indicative of good sludge settleability, while values exceeding 150 mL/g may suggest deteriorating settling characteristics or bulking conditions [1].

2.5.5 Mixed Liquor Suspended Solids (MLSS)

MLSS represents the total concentration of suspended solids in the biological reactor, including active biomass and inert solids. MLSS concentrations vary depending on the treatment zone and process configuration [1].

Table 6. Typical MLSS concentrations [1]

Process unit	Typical MLSS (mg/L)
Denitrification	2,000–4,000
Nitrification	3,000–5,000
MBR	6,000–12,000

2.5.6 Dissolved Oxygen (DO)

Dissolved oxygen is a critical parameter for aerobic biological treatment and nitrification. DO concentration in the aeration tank should be maintained at 1.5 to 2.5 mg/L to sustain aerobic biological activity. A minimum DO of 0.7 mg/L is required to initiate nitrification, while higher DO concentrations of 2.0 to 3.0 mg/L provide a small additional increase in nitrification rates. DO values above 4 mg/L result in little or no improvement in performance but significantly increase aeration energy costs and can promote the growth of foaming organisms [1]. For denitrification, anoxic zones with DO ≈ 0 mg/L are maintained, where nitrate serves as the electron acceptor.

Nitrification requires strict aerobic conditions and is sensitive to several environmental factors. The typical operating conditions required for effective nitrification are summarized in Table 7 [1].

Table 7. Typical operating condition for nitrification tank [1]

Parameter	**Typical Range**
DO	1.5–3 mg/L
pH	6.5–8.5
Temperature	10–35°C
MLSS	2,000–5,000 mg/L

Denitrification takes place under anoxic conditions and is monitored using oxidation-reduction potential (ORP). The optimal ORP range for denitrification is −50 to −150 mV. The relationship between ORP values and process conditions is summarized in Table 8.

Table 8. ORP conditions for denitrification [1]

ORP Range	**Condition**
+100 to +400 mV	Oxidizing condition
0 to +100 mV	Transition zone
-50 to -150 mV	**Ideal for denitrification**
<-200 mV	Can lead to unwanted processes like sulfate reduction, odor issues

3. Methodology

3.1 Khaanzaa Wastewater Treatment Plant

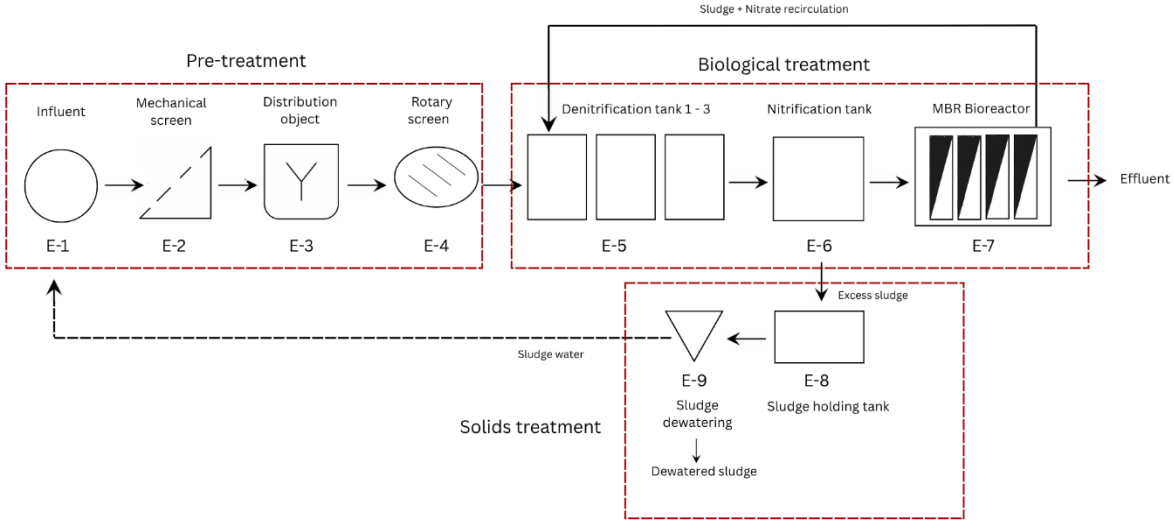


Figure 10. Flowsheet of Khaanzaa WWTP

The Khaanzaa wastewater treatment plant, operated by Khaanzaa LLC under subcontract with the Oyu Tolgoi mining project in the Gobi region of Mongolia, is designed as a membrane bioreactor (MBR)-based facility for domestic wastewater treatment. The plant serves the residential and operational workforce of the mining site and is configured with two parallel treatment trains to provide operational flexibility under varying hydraulic and organic loading conditions. The current design capacity is 6,000 population equivalent (EP), with an expansion provision of up to 8,000 EP [2].

The hydraulic design is based on an average per capita wastewater generation rate of 207 L/EP·day, corresponding to design average dry weather flows of approximately 1,240 m^3/day at 6,000 EP and 1,656 m^3/day at 8,000 EP. This relatively high per capita value reflects site-specific conditions, including additional water contributions from mining-related activities and service facilities [2].

Each of the two parallel bioreactor trains comprises three anoxic denitrification tanks, one aerobic nitrification tank, and one MBR membrane tank. A total of six denitrification tanks are installed, three per train, with a combined volume of 414 m^3 and an individual working volume of approximately 69 m^3 per tank. Mixing within the denitrification tanks is provided by submersible mixers operating under anoxic conditions, where facultative anaerobic

bacteria reduce nitrate to nitrogen gas using biodegradable COD as the carbon source. The aerobic nitrification stage consists of two tanks, one per train, with a total volume of 729 m^3, where ammonia nitrogen is oxidized to nitrate by autotrophic nitrifying bacteria under continuously aerated conditions. Nitrate-rich mixed liquor is recirculated from the nitrification zone back to the denitrification tanks to sustain the biological nitrogen removal cycle. The MBR system consists of two membrane tanks, one per treatment train, with a combined total volume of 82 m^3. Each membrane tank contains 4 cassettes, with each cassette comprising 15 hollow fibre membrane modules manufactured by Memstar (Singapore), resulting in a total of 60 modules per tank and 120 modules across both treatment trains [2].

Preliminary treatment is provided by a multi-stage screening system designed to protect downstream biological processes and minimize membrane fouling risk. Coarse solids larger than 5 mm are removed by mechanical fine screens, while finer suspended materials are captured by rotary screens with openings of approximately 1.7 mm. The screened wastewater is then pumped to the biological treatment stage through a distribution chamber equipped with variable speed submersible pumps. Membrane fouling is managed through an integrated physical and chemical cleaning program. Periodic backwashing using sodium hypochlorite (NaOCl) is applied to restore membrane permeability following fouling accumulation. Membrane performance is continuously monitored through permeability, expressed in LMH/bar [2]. Rather than measuring TMP directly, the SCADA system automatically calculates permeability from real-time flux and pressure readings, providing a direct indicator of membrane condition. A progressive decline in permeability indicates fouling accumulation and the need for cleaning. Based on operational data collected from the Khaanzaa WWTP over the study period, further analysis was conducted to evaluate treatment efficiency and to investigate the influence of key operational parameters including HRT, SRT, MLSS, DO, permeate flux on MBR system performance.

Site Visit to Khaanzaa Wastewater Treatment Plant (WWTP)

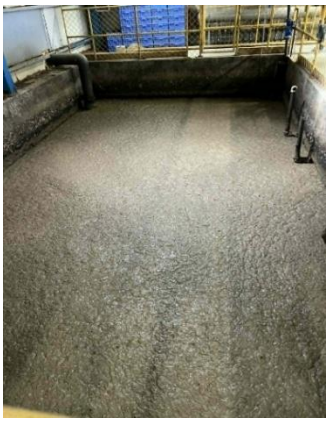


Figure 11. Nitrification Tank

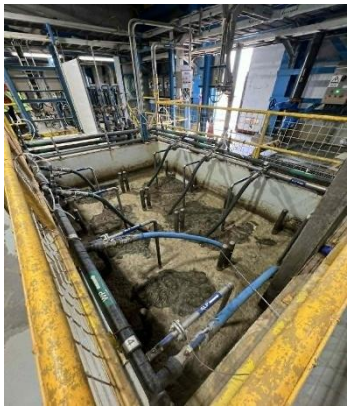


Figure 12. Denitrification Tank



Figure 13. ORP sensor installation





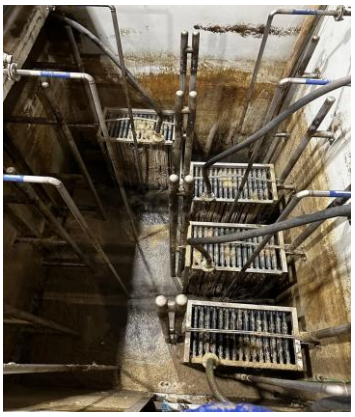


Figure 14. Membrane Bioreactor (MBR) tanks during operation and maintenance



Figure 15. Dewatered sludge with moisture content of 80–85%



Figure 16. Online multiparameter sensor



Figure 17. Permeate sample



Figure 18. Control panel



Figure 19. Screw press filter for sludge dewatering

3.2 Data collection

Operational data from the Khaanzaa Wastewater Treatment Plant (WWTP) were collected from January 1, 2024 to February 11, 2026 covering a continuous monitoring period of approximately 25 months, to evaluate the performance and process efficiency of the plant's membrane bioreactor (MBR) system. The dataset comprises five categories, integrating laboratory-based chemical analyses with continuously recorded automated sensor data across key stages of the treatment process.

Influent and effluent water quality parameters were determined through laboratory analysis conducted twice per week at the Khaanzaa WWTP on-site laboratory, following standard methods for the examination of water and wastewater. A full one-year record for 2025 was compiled from these biweekly measurements, with sample sizes ranging from n = 33 to n = 82 per parameter. Key indicators measured include biochemical oxygen demand (BOD), chemical oxygen demand (COD), total suspended solids (TSS), ammonium (NH_4^+), total nitrogen (TN), and phosphate (PO_4^{3-}), across both influent and effluent streams.

Continuous daily flow and sludge process data were obtained from the plant's automated monitoring system for the full 2024–2025 period. Parameters recorded include influent and effluent daily volumetric flow rates (m^3/day), sludge removed during the biological treatment process from Train A and Train B (m^3/day), sludge transferred to the dewatering unit (m^3/day), and decanted water volume following dewatering (m^3/day). Nitrification tank parameters including mixed liquor suspended solids (MLSS, mg/L), dissolved oxygen (DO, mg/L), pH, and temperature (°C) were also logged continuously for both Train A and Train B. Membrane permeability (LMH/bar) was recorded for each module across both treatment trains (A1–A4 and B1–B4), with monthly average values compiled per module and per train to assess fouling progression and inter-module variability over time. Chemical consumption associated with membrane cleaning operations was recorded for the same period, tracking sodium hypochlorite (NaClO) usage for backwash and cleaning cycles.

3.3 Sample Collection

Wastewater samples were collected from five sampling points within the Khaanzaa WWTP on March 10, 2026, covering the following treatment stages: influent, denitrification tank, nitrification tank, MBR tank, and final effluent. Samples were collected to characterize wastewater quality across all major treatment stages and to evaluate the removal efficiency of each process unit.

The collected samples were transported to the Chemical Research Institute in Ulaanbaatar on March 11, 2026. The samples were retrieved from the laboratory on March 12, 2026 and stored at 4–5°C in the GMIT Environmental Engineering Laboratory prior to analysis. Laboratory analyses commenced on March 16, 2026. MLSS and MLVSS were measured three times over the study period, on March 20, April 7, and April 13, 2026.

3.4 Parameters Measured

Laboratory analyses were conducted to determine the following parameters: biochemical oxygen demand (BOD_5), chemical oxygen demand (COD), total nitrogen (TN), total phosphorus (TP), total iron (Fe), sulfate (SO_4^{2-}), and mixed liquor suspended solids (MLSS/MLVSS).

3.4.1 Chemical Oxygen Demand (COD)

COD was determined using the closed reflux titrimetric method in accordance with Standard Methods Section 5220 C. A measured volume of sample was digested with potassium dichromate ($K_2Cr_2O_7$) in the presence of sulfuric acid (H_2SO_4) and silver sulfate (Ag_2SO_4) as a catalyst at 150°C for 2 hours in a block digester. After cooling, the excess dichromate was titrated with ferrous ammonium sulfate (FAS) using ferroin as an indicator. The endpoint was identified by a sharp color change from blue-green to reddish-brown. COD was calculated as follows:

$$COD\ as \frac{mg}{L}\ O_2 = \frac{(A-B)\ \times M \times 8000}{mL\ of\ sample} \quad (3.1)$$

where A is the mL FAS used for blank, B = mL FAS used for sample, M is the molarity of FAS, and 8000 is the milliequivalent weight of oxygen x 1000 mL/L

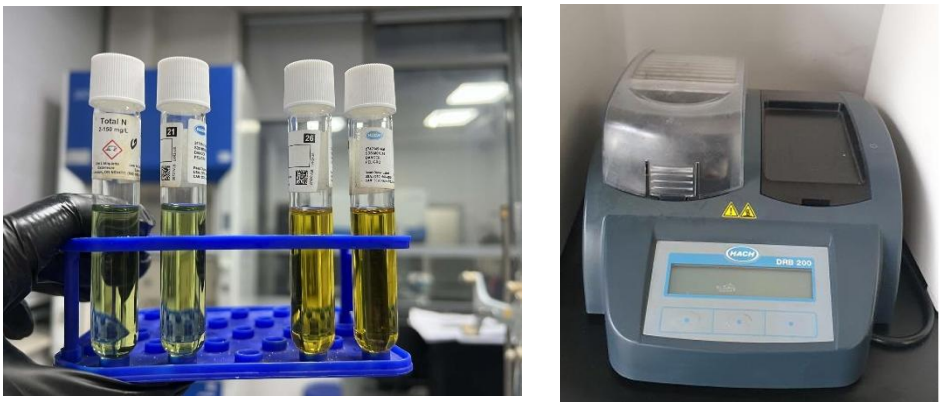


Figure 20. Apparatus Used for COD Determination, A. Test tube 10mm x 80mm B. Hach DRB 200, DRB 200

3.4.2 Biochemical Oxygen Demand (BOD_5)

BOD_5 was measured using the Lovibond BOD System model 600. This instrument measures the amount of dissolved oxygen microorganisms consume over a 5-day incubation period at 20°C in the dark. Samples were selected within the required measurement range, and reagents were used according to the manufacturer's instructions in the equipment manual.



Figure 21. Apparatus used for Biochemical Oxygen Demand, BD600

3.4.3 Total Nitrogen (TN)

Total nitrogen was determined using the TNT Persulfate Digestion Method (Hach Method 10071) with the DR/870 colorimeter. The DRB200 reactor was preheated to 103–106°C. Two millilitres of sample were added to a Total Nitrogen Persulfate Reagent vial together with a Total Nitrogen Hydroxide Reagent Powder Pillow and digested for 30 minutes. After

cooling, TN Reagent A and B Powder Pillows were added sequentially with defined reaction periods of 3 and 2 minutes respectively. The absorbance was measured using the DR/870 colorimeter and the result was displayed directly in mg/L N.

3.4.4 Total Iron (Fe)

Total iron was determined using the FerroVer Method (Hach Method 8008), a USEPA-approved method for reporting wastewater analysis. A 10 mL sample was placed in a sample cell and one FerroVer Iron Reagent Powder Pillow was added. The cell was capped and inverted to dissolve the reagent. A 3-minute reaction period was allowed, during which an orange color develops in proportion to the iron concentration. Absorbance was measured and results were reported in mg/L Fe.

3.4.5 Sulfate (SO_4^{2-})

Sulfate was determined using the SulfaVer 4 Turbidimetric Method (Hach Method 8051). A 10 mL sample was placed in a sample cell and one SulfaVer 4 Sulfate Reagent Powder Pillow was added. The cell was capped, inverted several times to mix, and allowed to react for 5 minutes. The white turbidity that develops is proportional to the sulfate concentration. Absorbance was measured and results were reported in mg/L SO_4^{2-}.

3.4.6 Total Phosphorus (TP)

Total phosphorus was determined using the PhosVer 3 with Acid Persulfate Digestion method (Hach Method 8190). A 5.0 mL sample was added to a Total Acid Hydrolyzable Test Vial with a Potassium Persulfate Powder Pillow and digested in the DRB200 reactor at 150°C for 30 minutes. After cooling, 2.0 mL of 1.54 N sodium hydroxide was added to neutralize the sample. PhosVer 3 Phosphate Reagent Powder Pillow was then added and the sample was allowed to react for 2 minutes. The resulting blue color, proportional to phosphate concentration, was measured at 880 nm using the DR/870 colorimeter and reported in mg/L PO_4^{3-}.



Figure 22. Hach DR/870 Portable Colorimeter.

3.4.7 Mixed Liquor Suspended Solids (MLSS) and Volatile Suspended Solids (MLVSS)

MLSS and MLVSS were determined gravimetrically in accordance with Standard Methods. A well-mixed sample was filtered through a pre-weighed glass fibre filter. The filter was dried at 103–105°C to constant weight for MLSS determination. MLSS was calculated as:

$$MLSS = \frac{Mass\ of\ filter\ after\ evaporation\ at\ 100°C\ (g) - Mass\ of\ filter}{Sample\ volume\ (ml)} \times 1{,}000{,}000\ (mg/l) \qquad (3.2)$$

For MLVSS determination, the dried filter was subsequently ignited at 550°C for 15–20 minutes in a muffle furnace. The loss on ignition represents the volatile (organic) fraction of the suspended solids:

$$MLVSS = \frac{Mass\ of\ filter\ after\ evaporation\ at\ 550°C\ (g) - Mass\ of\ filter}{Sample\ volume\ (ml)} \times 1{,}000{,}000\ mg/l \qquad (3.3)$$



Figure 23. Evaporation dishes after drying at 103–105°C (MLSS analysis)

3.5 Statistical Analysis

To characterise the variability and central tendency of the collected operational data, descriptive statistical analyses were performed on all key parameters. The following statistical measures were calculated for each dataset [7]:

The arithmetic mean ($\bar{x}$) was calculated as:

$$\bar{x} = \frac{\Sigma x_i}{n} \tag{3.4}$$

The sample standard deviation (s) was computed as:

$$s = \sqrt{\frac{\sum(x - \bar{x})^2}{n - 1}} \tag{3.5}$$

The standard error of the mean (SE) was determined as:

$$SE = \frac{s}{\sqrt{n}} \tag{3.6}$$

To express the uncertainty around the mean, the 95% confidence interval (CI) was calculated as:

$$CI = \bar{x} \pm t \times \frac{s}{\sqrt{n}} \tag{3.7}$$

n	t
2	12.71
3	4.30
4	3.18
5	2.78
10	2.26
∞	1.96

where s is the sample standard deviation, n is the number of observations, and t is the critical value of the Student's t-distribution at the 95% confidence level [7].

The relative variability of each parameter was quantified using the coefficient of variation (CV), expressed as a percentage:

$$CV(\%) = \frac{SE}{\bar{x}} \times 100 \tag{3.8}$$

These statistical descriptors were applied uniformly across all laboratory-measured and automatically recorded datasets to enable systematic comparison of operational variability between parameters, treatment trains, and monitoring years.

The increase in sludge wasting rate was modeled using an exponential growth equation:

$$Q_t = Q_0 \times (r)^t \quad (3.9)$$

$$t = \frac{ln(Q_t/Q_0)}{ln(1+r)} \quad (3.10)$$

where Q_t is the sludge wasting rate at time t (m³/day), Q_0 is the initial sludge wasting rate (m³/day), r is the daily growth rate, and t is the time (days).

4. Result and Discussion

4.1 Determination of Key Operational Parameters

The hydraulic retention time (HRT) and sludge retention time (SRT) of the Khaanzaa WWTP were determined using Equations (2.21) and (2.22), respectively. Based on the operational data, the total system HRT was calculated as 0.799 days (19.18 hours), while the SRT was determined to be 32.18 days.

Table 9. Hydraulic retention time (HRT) and sludge retention time (SRT) for each treatment unit

Tank	Volume (m³)	Each tank volume (m³)	HRT (days)	HRT (hours)	SRT (days)
Denitrification	414	69	0.270	6.48	12.73
Nitrification	729	365	0.476	11.42	17.57
MBR Bioreactor	82	41	0.053	1.27	2
Total System	1225	613	0.799	19.18	32.18

4.1.1 Temperature-Corrected Kinetic Parameters

Standard kinetic coefficients for biological treatment processes at 20°C were obtained from Table 3 and adjusted to the operating temperature of 12°C using the van't Hoff–Arrhenius equation (Eq. 2.16).

The temperature correction resulted in a decrease in the maximum specific growth rate (μmax) and slight variations in the half-saturation constant (Ks), reflecting the reduced biological activity under lower temperature conditions. This reduction is particularly significant for nitrification, as autotrophic bacteria are highly sensitive to temperature changes.

Table 10. Temperature correction of standard kinetic coefficients for COD oxidation and NH_4^+ oxidation

Parameter	Unit	θ	COD (20°C)	COD (12°C)	θ	NH_4^+ (20°C)	NH_4^+ (12°C)
μmax	d^{-1}	1.07	6.0	3.492	1.07	0.9	0.516
Ks	mg/L	1.04	8.0	5.846	1.04	0.5	0.393
kd	d^{-1}	1.00	0.12	0.12	1.00	0.17	0.17

4.1.2 Calculation Based on Monod Kinetics

Using the Monod-based design equations (Eq. 2.9–2.15), theoretical values of effluent substrate concentration, biomass concentration, growth rates, and F/M ratio were calculated for both COD and ammonia removal at 20°C and 12°C. The calculations were performed using average influent and effluent concentrations obtained from the 2025 operational dataset, where the influent COD (S_0) was 441.5 mg/L, the effluent COD (S) was 16.3 mg/L, the influent NH_4^+ concentration was 76.06 mg/L, and the effluent NH_4^+ concentration was 1.18 mg/L.

The detailed calculations are presented in Appendix B, while the summarized results are shown in Table 11.

Table 11. Summary of theoretical kinetic parameters for COD and NH_4^+ removal at 20°C and 12°C

Parameter	Unit	COD 20°C	COD 12°C	NH_4^+ 20°C	NH_4^+ 12°C
Theoretical effluent substrate S	mg/L	0.56	0.74	0.169	0.308
Biomass conc. X (Nitrification)	mgVSS/L	2272	2272	104	104
Net biomass yield Y_{net}	gVSS/g	0.144	0.144	0.0376	0.0376
Specific growth rate μ	d^{-1}	4.03	2.571	0.632	0.387
Net specific growth rate μ_{net}	d^{-1}	3.91	2.451	0.462	0.217
F/M ratio	gCOD/gVSS·d	0.147	0.147	—	—
Min. SRT for nitrification	days	—	—	1.37	2.89
Verified SRT (1/SRT check)	days	17.5	—	17.5	—

4.1.3 Biomass Mass balance

To verify the internal consistency of the system and determine the recirculation sludge concentration entering the denitrification zone, a biomass mass balance was performed

across the treatment system using Equation (2.23). The calculation was based on measured influent, effluent, waste sludge, and internal recirculation flow rates, along with their corresponding biomass concentrations.

By substituting the known operational data, it was found that the total solids load entering the system did not balance with the solids leaving through the effluent and waste sludge streams alone. This imbalance indicates the presence of a significant internal recirculation solids load within the system. Rearranging Equation (2.23) to determine the recirculation sludge concentration, X_r was calculated to be approximately 7110 mg/L, indicating that a relatively high concentration of mixed liquor suspended solids is returned from the MBR tank to the denitrification zone. The recirculation flow rate of was estimated based on an average return flow of 80 m³/h operating continuously over 24 hours. See Appendix C for detailed calculations.

4.2 Laboratory Results

Table 12. BOD Measurement Over 5 days

	Day 1	Day 2	Day 3	Day 4	Day 5
Influent sample BOD bottle 4 (mg/L)	33	57	131	166	178
Influent sample BOD bottle 6 (mg/L)	97	116	82	94	138
Effluent sample BOD bottle 1 (mg/L)	Underrange	4	6	9	17
Effluent sample BOD bottle 5 (mg/L)	Underrange	16	17	23	31

Table 13. Total Nitrogen & Total Phosphate

	Influent 1	Influent 2	Effluent 1	Effluent 2
Total Nitrogen TN (mg/L)	56	55	11.3	9.9
Phosphate (PO4) TP (mg/L)	18.65	19.55	0.56	0.51

Table 14. Sulfate & Iron

	Sulfate (SO4) $(\frac{mg}{l})$	Mean	Iron (Fe) $(\frac{mg}{l})$	Mean
Influent 1	390	395	0.36	3.5
Influent 2	400		0.34	

Denitrification 1	440	450	49.1	50.2
Denitrification 2	460		51.3	
Nitrification 1	645	650	35.5	36.33
Nitrification 2	655		37.1	
MBR 1	248	250	6.7	6.9
MBR 2	252		7.1	
Effluent 1	670	680	0.10	0.105
Effluent 2	690		0.11	

Table 15. Chemical oxygen demand (COD)

COD ($\frac{mg}{l}$)		**Mean**
Influent 1	192	176
Influent 2	160	
Effluent 1	32	32
Effluent 2	32	

Table 16. MLSS and MLVSS concentrations

	MLSS ($\frac{mg}{l}$)		**MLVSS** ($\frac{mg}{l}$)	
Influent 1	400	500	200	200
Influent 2	600		200	
Denitrification 1	9400	9700	2000	2100
Denitrification 2	10000		2200	
Nitrification 1	7600	7600	1600	1600
Nitrification 2	7600		1600	
MBR 1	7200	7200	1800	1900
MBR 2	7200		2000	
Effluent 1	400	400	200	200
Effluent 2	400		200	

4.3 Sludge Characteristics and Observation



Figure 24. Visual comparison of sludge samples from different treatment units

Wastewater samples collected from the Khaanzaa WWTP were visually examined across five treatment stages: influent, denitrification tank, nitrification tank, MBR tank, and final effluent. As shown in Figure 24, the samples are arranged sequentially from left to right. A notable observation was the black coloration of sludge in the denitrification, nitrification, and MBR units.

Possible Causes of Black Sludge Formation

The black coloration of sludge was hypothesized to be associated with sulfide formation under anaerobic micro-conditions within the biological reactors. Under insufficient aeration or mixing, localized anaerobic zones may develop, enabling sulfate-reducing bacteria to convert sulfate (SO_4^{2-}) into hydrogen sulfide (H_2S):

$$SO_4^{2-} + 2CH_2O \rightarrow H_2S + 2HCO_3^- \quad (3.11)$$

The produced H_2S can subsequently react with dissolved iron (Fe^{2+}), forming iron sulfide (FeS), a black precipitate:

$$Fe^{2+} + H_2S \rightarrow FeS \downarrow \quad (3.12)$$

This mechanism explains the observed dark coloration of sludge.

Laboratory analysis of the collected samples indicated that the influent sulfate concentration was approximately 365 mg/L, which is within the Mongolian standard limit (MNS 6561: ≤700 mg/L), while the influent iron concentration was around 3.5 mg/L, slightly exceeding typical reference values. The effluent iron concentration was measured at 0.105 mg/L, remaining within the discharge standard (MNS 4943). The simultaneous presence of sulfate and iron suggests favorable conditions for iron sulfide (FeS) formation under reducing environments, which may contribute to the observed black coloration of sludge.

During laboratory observations, the sludge exhibited poor settling characteristics, and the sludge volume index (SVI) could not be determined due to the absence of settling. This behavior may be attributed to factors such as high sludge retention time (SRT), leading to aged sludge, as well as the presence of fine, dispersed or colloidal biomass structures that inhibit floc formation and settling.

Effect of Sample Storage on Results

It is important to note that the samples were analyzed approximately 5 days after collection, whereas biological wastewater analysis is typically conducted within 24 hours to preserve sample integrity. In particular, sludge settleability tests such as the sludge volume index (SVI) are required to be performed immediately after sampling (typically within 1–2 hours), as delays can significantly alter floc structure and settling behavior. During this extended storage period, oxygen depletion may have occurred, creating localized anaerobic conditions within the samples and promoting additional sulfide formation.

This interpretation is supported by field observations made during a site visit to the Khaanzaa WWTP on April 24, 2026, where sludge in the nitrification tank appeared brown, indicating normal and healthy activated sludge conditions. Therefore, the previously observed black coloration and poor settling behavior are likely influenced by post-sampling transformations rather than representing the actual operational condition of the treatment plant. These findings emphasize that biological wastewater samples are highly time-sensitive, and delays in analysis can significantly alter sludge characteristics, potentially leading to misinterpretation of treatment performance.

4.4 Operational Data Analysis and Performance Evaluation

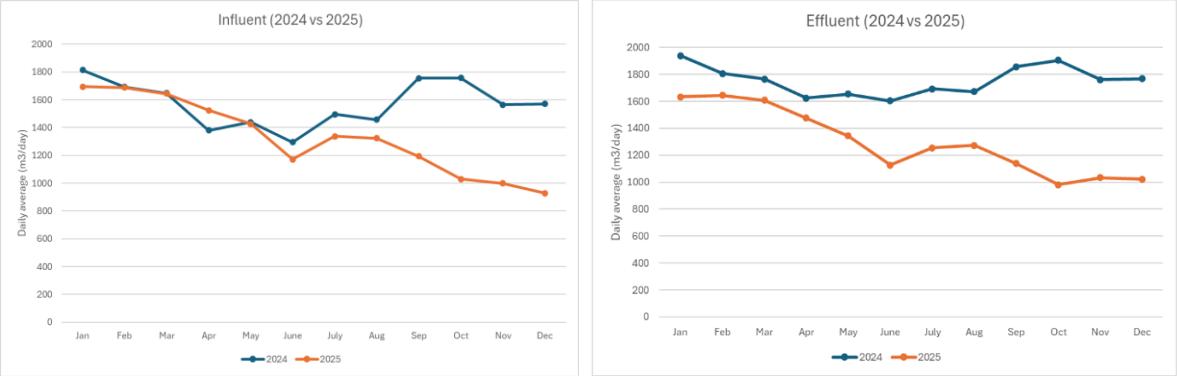


Figure 25. Comparison of Monthly Influent and Effluent Flow Rates (2024–2025)

A comparison of monthly influent and effluent flow rates between 2024 and 2025 indicates a noticeable difference in wastewater volume trends. In 2024, the influent flow generally increased toward the end of the year, reaching higher values during the autumn and early winter months. In contrast, the influent flow in 2025 shows a decreasing trend over the same period. Specifically, when comparing December values, the influent flow in 2025 was approximately 600 m³/day lower than in December 2024. This suggests an overall reduction in wastewater generation or water consumption in 2025 compared to the previous year.

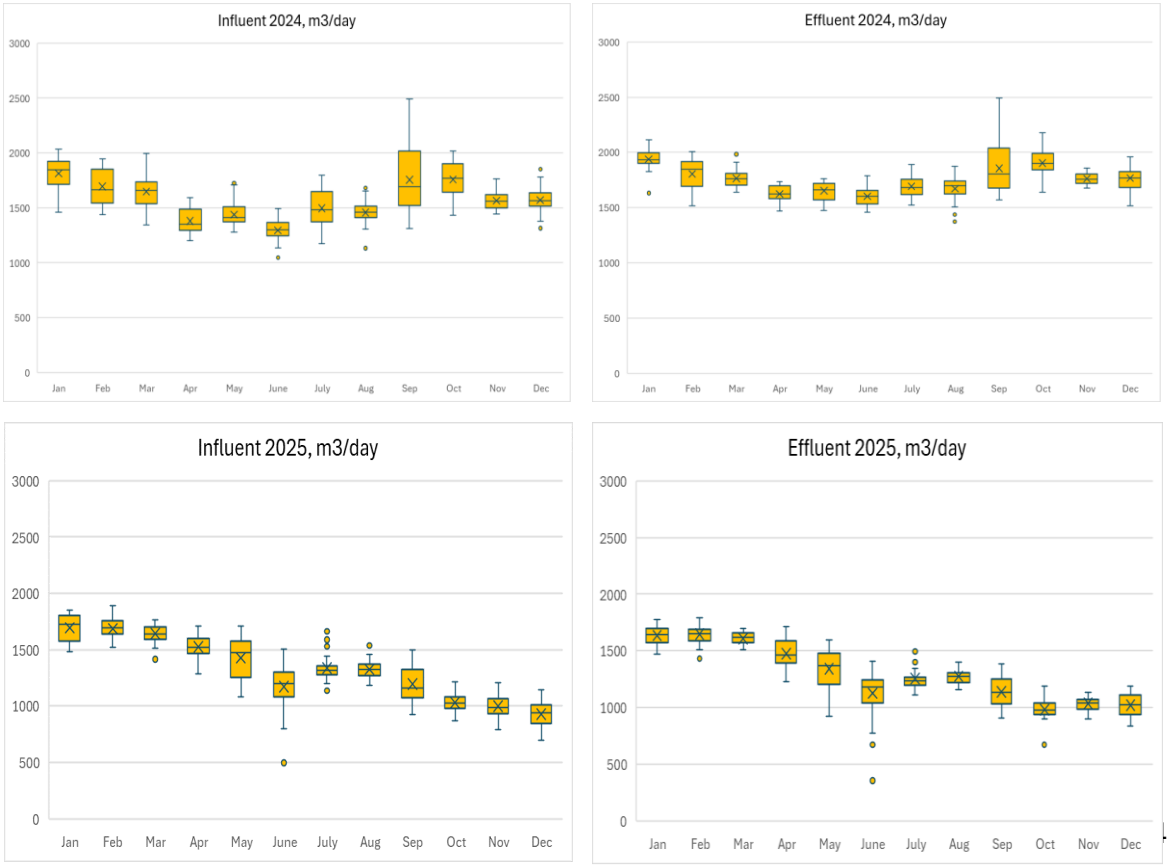


Figure 26. Monthly Distribution of Influent and Effluent Flow Rates Using Boxplot

The boxplot analysis reveals that influent and effluent flow rates in 2024 exhibit higher variability compared to 2025, particularly during the late summer and autumn months. In contrast, the 2025 data show a more stable but consistently lower flow regime throughout the year. The median flow values in 2025 are noticeably lower than those in 2024 for both influent and effluent, confirming an overall reduction in wastewater volume. A seasonal increase in flow is observed in 2024 toward September–October, whereas 2025 demonstrates a gradual decline over the same period.

Table 17. Wastewater characteristics of lab determination 2025

		Mean, mg/L	Max, mg/L	Min, mg/L	Std.dev	±t*std.dev/n^0.5
Ammonium (NH4+)	Influent, n=78	76.09	100	21	23.68	**± 5.3**
	Effluent, n=82	1.18	10	0.2	2.28	**± 0.5**
Total Nitrogen	Influent, n=81	102.9	198	5	41.9	**± 9.27**
	Effluent, n=59	12.27	22	0.3	5.84	**± 1.52**
Phosphate (PO4-)	Influent, n=77	9.14	15	2.4	4.25	**± 0.96**
	Effluent, n=79	2.71	7.1	0.2	1.7	**± 0.38**
COD	Influent, n=82	441.54	614	130	160.72	**± 35.32**
	Effluent, n=67	16.31	46	2	7.24	**± 1.76**
MLSS	Influent, n=82	6332.38	14500	240	2269.86	**± 498.81**
	Effluent, n=82	6332.38	14500	240	2269.86	**± 498.81**
BOD	Influent, n=33	195.61	406	2	95.67	**± 33.92**
	Effluent, n=33	3.74	18.3	0	3.48	**± 1.24**
TSS	Influent, n=81	382.99	1310	76	212.77	**± 47.04**
	Effluent, n=81	14.17	50	0	10.81	**± 2.39**

Table 18. Daily Sensor Data for Nitrification Tank

Parameter	MLSS 2024 (mg/L)		MLSS 2025 (mg/L)		DO 2024 (mg/L)		DO 2025 (mg/L)	
	Train A	Train B	Train A	Train B	Train A	Train B	Train A	Train B
Mean	5757	6316.5	6183	5561.8	1.8	1.9	2.5	2
Std Dev	938	1337	2065	1906.2	1.3	1.5	1.5	1.3
Max	9125	10536	13094	13156	9.7	9.4	11.7	7
Min	3128	3281	1125	0	0	0	0.2	0

CV (%)	16.3	21.2	33.4	34.3	72.2	78.9	60	65

The analysis of MLSS concentrations in the nitrification tanks (Train A and Train B) for 2024 and 2025 indicates significant temporal variability. In 2024, the average MLSS values were 5757 mg/L (Train A) and 6316.5 mg/L (Train B), while in 2025, the averages were 6183 mg/L (Train A) and 5561.8 mg/L (Train B). These values are generally within or slightly above the typical operational range for nitrification processes (3000–5000 mg/L), indicating relatively high biomass concentrations.

However, substantial fluctuations are observed in both years. In 2024, MLSS ranged from 3128 to 9125 mg/L (Train A) and 3281 to 10536 mg/L (Train B). In 2025, the variation became even more pronounced, with values ranging from 1125 to 13094 mg/L (Train A) and 0 to 13156 mg/L (Train B). The high coefficient of variation (CV), particularly in 2025 (up to ~34%), confirms that MLSS levels were highly unstable.

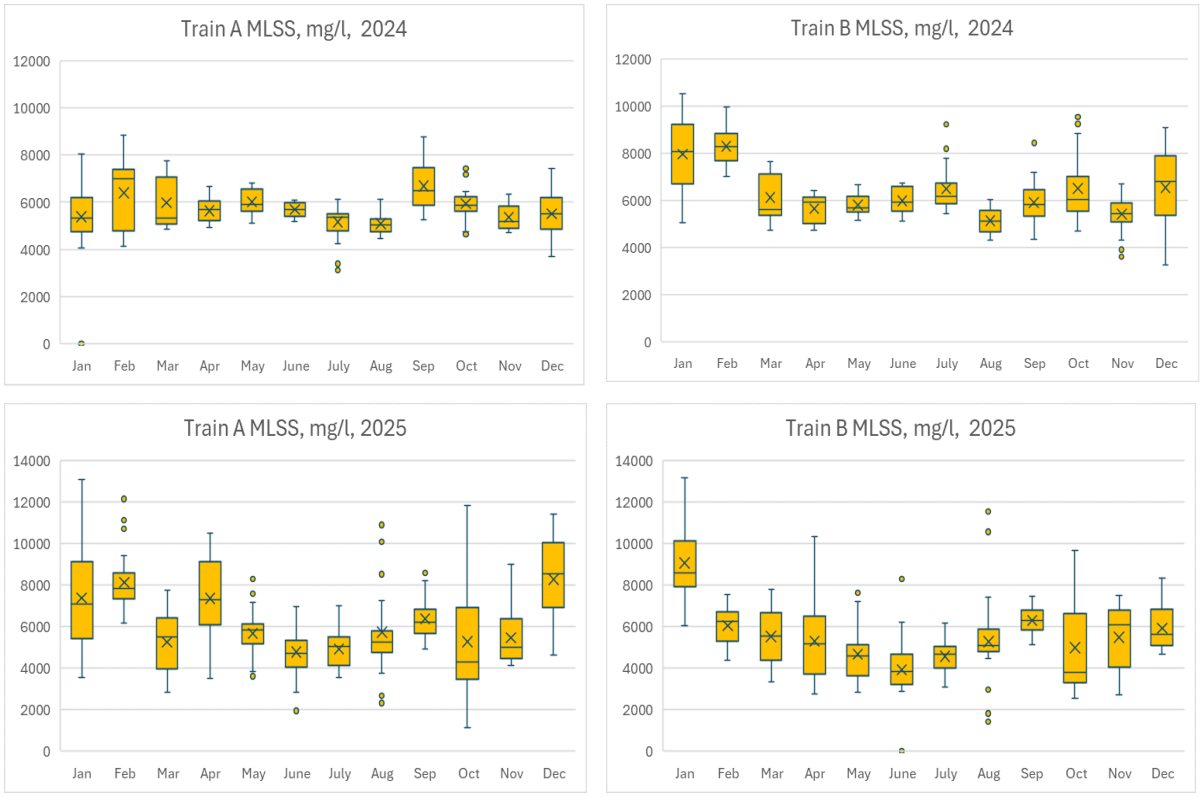


Figure 27. Monthly Variation of MLSS Concentrations in Nitrification Tanks

The boxplot analysis further illustrates this variability, showing wide interquartile ranges and the presence of multiple outliers across several months. This indicates inconsistent biomass distribution and fluctuating process conditions. The observed MLSS variability can be attributed to several operational and influent-related factors. The Khaanzaa WWTP receives transported wastewater from multiple sources within the Oyu Tolgoi site, including concrete production facilities, vehicle maintenance areas, explosive material handling units, and washing systems. Such heterogeneous influent characteristics can lead to fluctuations in organic loading and solids concentration, directly affecting MLSS levels. Additionally, operational practices such as foam removal from the nitrification tanks were reported to influence MLSS concentrations, contributing to biomass loss and further variability.

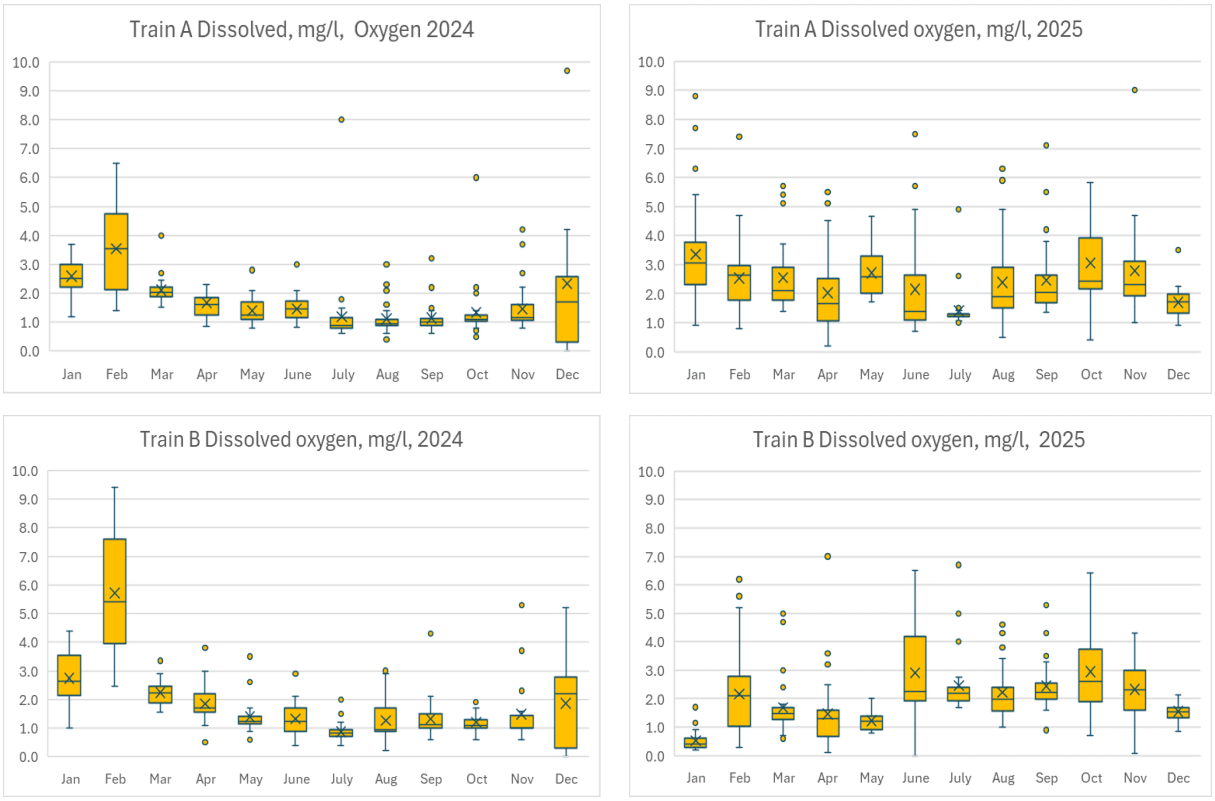


Figure 28. Monthly Variation of DO Concentrations in Nitrification Tanks

The analysis of dissolved oxygen (DO) concentrations in the nitrification tanks for both Train A and Train B during 2024–2025 indicates significant variability and suboptimal control conditions. The typical DO range required for effective nitrification is 1.5–2.5 mg/L, which is sufficient to sustain aerobic microbial activity while minimizing energy consumption. However, the observed DO values frequently deviated from this optimal range. In both years, DO concentrations occasionally reached values as high as 9 mg/L, indicating over-aeration.

Such excessive DO levels do not significantly improve nitrification efficiency but result in unnecessary energy consumption due to excessive air supply. At the same time, DO concentrations in several instances dropped close to 0 mg/L, suggesting temporary oxygen limitations that could negatively impact nitrification performance. The presence of both extremely high and very low DO values indicates unstable aeration control.

The boxplot analysis further confirms this observation, showing a wide distribution range and numerous outliers across multiple months. In 2024, relatively stable DO levels were observed during mid-year (May–September), whereas higher fluctuations occurred in early and late months. In contrast, 2025 exhibits consistently higher variability, with frequent deviations above and below the optimal range.

Periods of Excessive Aeration (DO > 3.0 mg/L)

Using 3.0 mg/L as the over-aeration threshold, the monitoring data revealed that both treatment trains experienced frequent exceedance events. In 2024, Train A exceeded 3.0 mg/L on 38 days and Train B on 53 days, totaling 91 train-days of over-aeration across 365 days of operation. In 2025, exceedance days increased markedly. Train A recorded 85 days and Train B 53 days, giving 138 train-days, a 52% increase compared to 2024.

The most severe episode occurred in February 2024, when Train B consistently recorded DO between 7.6 and 9.4 mg/L over multiple consecutive days. The single worst day was February 14, 2024, when Train A registered 6.4 mg/L and Train B 9.4 mg/L simultaneously, resulting in a combined excess energy loss of 5.36 kWh in one day. In 2025, October was the most problematic month, with Train A exceeding 3.0 mg/L on 14 days and Train B on 13 days, generating 19.85 kWh of excess consumption for that month alone.

Excess energy consumption was estimated using the surplus DO above 3.0 mg/L, an aeration tank volume of 729 m^3, and a coefficient of 1.5 kWh/kg O_2. Total excess energy in 2024 was 90.1 kWh, rising to 109.2 kWh in 2025, with a combined two-year total of 199.3 kWh. This 21.3% year-on-year increase reflects a worsening over-aeration trend. Since DO above 3–4 mg/L does not proportionally improve nitrification efficiency, this excess energy represents avoidable operational cost with no treatment benefit.

Table 19. Excess Aeration Energy Cost (2024–2025) [9]

Year	Excess Energy	Rate	Cost (₮)
2024	90.1 kWh	224 ₮/kWh	20,182 ₮

2025	109.2 kWh	280 ₮/kWh	30,576 ₮
Total	199.3 kWh	—	50,758 ₮

4.4.1 Statistical Analysis of Sludge Flow and Handling Data

The statistical analysis of daily flow and sludge handling data shows clear differences between 2024 and 2025. The average influent and effluent flows decreased from 1572.9 and 1753.87 m³/day in 2024 to 1327.6 and 1292.22 m³/day in 2025, indicating a reduction in overall hydraulic loading. Similarly, sludge production and handling volumes also declined in Table 19. The average sludge removed in process (A+B) decreased from 60.92 m³/day in 2024 to 46.92 m³/day in 2025, while sludge sent to dewatering reduced from 44.52 to 36.96 m³/day. The decanted water volume also decreased slightly from 23.83 to 21.8 m³/day.

Table 20. Descriptive Statistics of Sludge Flows (2024–2025)

Statistic parameter	Influent daily (m³/day)	Effluent daily (m³/day)	Remove in process (m³/day)			Sludge to pressed (m³/day)			Decanted after dewatering (m³/day)		
			A	B	A+B	A	B	A+B	A	B	A+B
Mean	1572.9	1753.87	28.63	34.02	60.92	19.85	26.42	44.52	13.15	15.17	23.83
Standard dev, S	218.9	155.16	13.87	18.16	23.98	11.7	15.32	16.39	8.24	10.67	14.7
Max	2489.94	2491	90	87.9	129	65	76	95	68	65.8	86
Min	1044.86	1372	0.7	0.6	0.6	1	1	1	0.1	0.1	0.1
CV (%) Coefficient of Variation	13.9	8.8	48.4	53.4	39.4	58.9	58	36.8	62.7	70.3	61.7

Statistic parameter	Influent daily (m³/day)	Effluent daily (m³/day)	Remove in process (m³/day)			Sludge to pressed (m³/day)			Decanted after dewatering (m³/day)		
			A	B	A+B	A	B	A+B	A	B	A+B
Mean	1327.6	1292.22	29.34	23.41	46.92	24.74	23.82	36.96	12.59	15.67	21.8
Standard dev, S	284.9	262.25	19.64	18.71	24.79	17.71	17.17	18.45	9.6	11.79	15.5
Max	1890.51	1792	99.9	99	126	80	70	80	60	65.4	102.2
Min	496.03	354	0.1	0.9	0.9	1	1	1	0.2	0.1	0.2
CV (%) Coefficient of Variation	21.5	20.3	66.9	79.9	52.8	71.6	72.1	49.9	76.3	75.2	71.1

4.4.2 Membrane Permeability Analysis

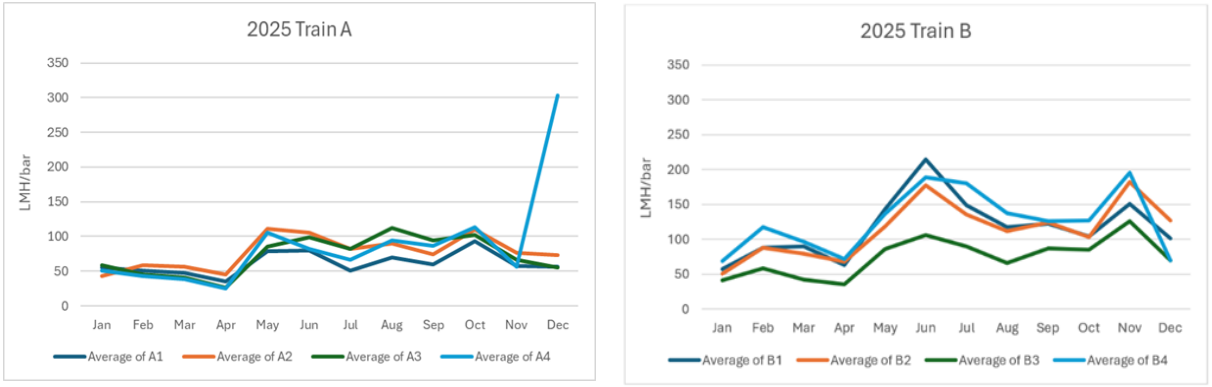


Figure 29. Monthly Average Membrane Permeability

Permeability 2025 Train A				
Months	**A1**	**A2**	**A3**	**A4**
Jan	55	43	59	51
Feb	51	59	45	43
Mar	47	56	40	38
Apr	35	45	27	25
May	79	111	85	106
Jun	80	105	99	82
Jul	50	82	82	66
Aug	70	90	112	94
Sep	59	74	94	87
Oct	93	110	102	113
Nov	58	77	66	56
Dec	56	73	55	303

Permeability 2025 Train B				
Months	**B1**	**B2**	**B3**	**B4**
Jan	57	51	41	69
Feb	88	88	59	117
Mar	90	79	43	97
Apr	63	68	35	72
May	143	119	86	137
Jun	215	178	106	189
Jul	149	136	90	180
Aug	118	112	67	138
Sep	123	124	87	126
Oct	105	103	85	127
Nov	151	182	126	195
Dec	102	127	70	70

As shown in Figure 29, membrane permeability in Train A values remained relatively stable during the first quarter (January–March), followed by a sharp increase in April–May. This sudden improvement is attributed to membrane maintenance and cleaning activities, where fouled membranes were removed and cleaned, resulting in improved permeability.

Following this, permeability gradually decreased, reaching a minimum of approximately 50 LMH/bar in July, indicating significant fouling and reduced membrane performance. This decline suggests that fouling accumulation occurred rapidly after cleaning. As a result, the frequency of cleaning and maintenance increased, with membrane servicing being conducted approximately every two months, indicating intensified operational intervention to sustain system performance. A significant increase in permeability was observed in December, reaching approximately 303 LMH/bar, which indicates membrane replacement. This sharp rise reflects the installation of new membrane modules, restoring permeability to a high level. In contrast, Train B shows relatively more stable permeability trends throughout the year, although fluctuations are still present. Peak values were observed during mid-year (June - July), followed by moderate declines, suggesting periodic fouling and partial recovery through routine cleaning.

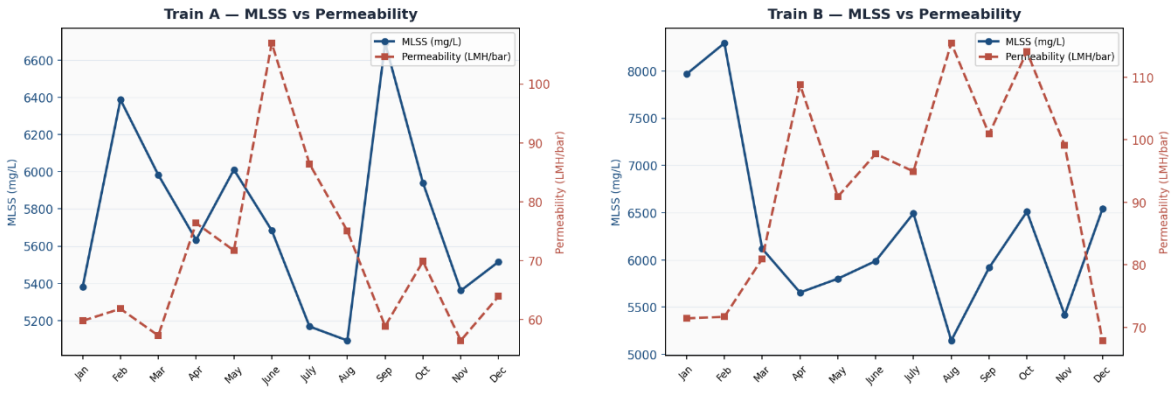


Figure 30. Relationship between MLSS and Membrane Permeability (2024)

As illustrated in Figure 30, the monthly analysis of 2024 data shows a **generally inverse relationship** between MLSS concentration and membrane permeability in both Train A and Train B. Periods of elevated MLSS are often associated with lower permeability values, indicating increased membrane fouling resistance.

In Train A, higher MLSS values observed in February and September correspond to reduced permeability, while lower MLSS levels during mid-year (June–July) coincide with slight improvements in permeability. Similarly, in Train B, increased MLSS concentrations during early and mid-year are linked with relatively lower permeability values. However, the relationship is not strictly linear, as fluctuations in permeability are also influenced by operational factors such as routine backwashing and periodic membrane cleaning. These interventions can temporarily improve permeability regardless of MLSS levels.

Table 21. Statistical Summary of Membrane Permeability

Membrane	2024					2025				
	Mean	Std Dev	Max	Min	CV (%)	Mean	Std Dev	Max	Min	CV (%)
A1	64.8	19.5	139	0	30.1	61.2	29.6	220	0	48.4
A2	68.7	19	137	0	27.7	77.3	36.5	350	0	47.1
A3	81	25.7	235	41	31.8	72.5	33.1	167	19	45.6
A4	67	18.7	160	0	27.9	89.3	90.9	610	20	101.8
B1	98.4	22	153	56	22.4	116.9	51.6	361	36	44.1
B2	90.6	20.1	210	36	22.2	113.8	48.8	312	20	42.9
B3	76.1	19.7	125	39	25.9	74.6	34.9	264	18	46.8
B4	106.3	24.4	190	53	22.9	126.3	86.4	939	7.8	68.4

4.4.3 Sludge Retention Time, Sludge Wasting, and Operational Recommendations

Analysis of the monitoring data revealed a clear inverse relationship between the daily sludge wasting flow rate (Qw) and sludge retention time (SRT). As Qw decreased, SRT increased, and when sludge wasting was stopped entirely, SRT increased sharply and uncontrollably. This pattern was consistently observed throughout the 2025 monitoring period, with SRT values fluctuating between approximately 11 and 138 days depending on the wasting regime applied as shown in Figure 31. The monthly average sludge removal (A+B, m³/day) and average SRT showed an opposing trend, confirming that inadequate or irregular sludge wasting is the primary driver of increased SRT at Khaanzaa WWTP.

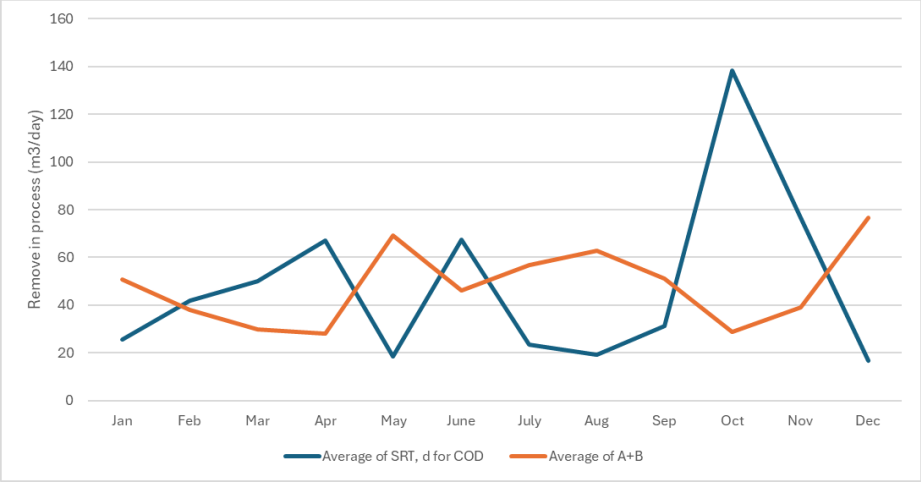


Figure 31. Relationship between SRT and Sludge Removal Rate (A+B), 2025

Operational Recommendation

To restore the sludge to a healthy, active state, an abrupt increase in Qw is not recommended, as sudden changes in sludge concentration would destabilize the microbial community and risk biomass washout. Instead, a gradual controlled wasting strategy is proposed, targeting the following conditions as the stable operating point with MLSS = 5,000 mg/L, SRT = 20 days, and Qw = 70 m^3/day.

Starting from the current condition where Qw is approximately 20 m^3/day, a daily 2% stepwise increase in wasting flow is recommended. Using Equation (3.10), the time required to increase the sludge wasting rate (Qw) from 20 m^3/day to 70 m^3/day at a 2% daily increment was calculated to be approximately 64 days. (see Appendix C for detailed calculations).

This gradual transition allows the biological system to adapt without causing shock to the microbial population. Over this approximately two-month period, MLSS is expected to progressively decline toward the target of 5,000 mg/L, and SRT will stabilize around 20 days, conditions that support active nitrification, adequate denitrification, and improved sludge settleability. Once this stable state is achieved, daily consistent sludge wasting at a fixed Qw is strongly recommended over intermittent or irregular wasting, as the data show that even brief interruptions in wasting caused rapid increase in SRT and sludge deterioration.

5. Conclusion

This study evaluated the operational performance of the membrane bioreactor (MBR) system at the Khaanzaa Wastewater Treatment Plant using both laboratory analysis and long-term operational data from 2024–2025. The results demonstrated that the MBR system is capable of achieving high treatment efficiency, with effective removal of COD and ammonia under the studied conditions. However, several operational challenges affecting system stability were identified. One of the key findings is the strong inverse relationship between sludge wasting (Qw) and sludge retention time (SRT). Insufficient or irregular sludge wasting resulted in excessively high SRT values (up to 138 days), leading to aged biomass, poor sludge settleability, and deterioration of biological performance. This condition was further associated with elevated MLSS concentrations and unstable process behavior.

Significant fluctuations in MLSS and dissolved oxygen (DO) were observed in both treatment trains, primarily due to variable influent characteristics and inconsistent operational control. DO concentrations frequently exceeded the optimal range (1.5–2.5 mg/L), resulting in unnecessary energy consumption, while occasional low DO conditions posed a risk to nitrification efficiency. Membrane performance analysis indicated that permeability was strongly influenced by fouling accumulation and maintenance practices. Periodic cleaning temporarily improved permeability. However, rapid fouling reoccurred, highlighting the importance of stable biological conditions in effective fouling control. Additionally, this study demonstrated that biological wastewater samples are highly time-sensitive. Delayed laboratory analysis significantly affected sludge characteristics, leading to misleading observations such as black sludge formation and poor settleability that were not representative of actual plant conditions.

Overall, the findings emphasize that stable operation of an MBR system requires proper control of key parameters, particularly sludge wasting, MLSS, SRT, and DO. Among these, sludge wasting was identified as the most critical factor governing biomass condition and overall process performance. Therefore, optimization of sludge management and aeration control is essential for improving system stability, reducing energy consumption, and enhancing long-term MBR performance.

Reference

1. Metcalf & Eddy, AECOM. Wastewater engineering: treatment and resource recovery. 5th ed. New York: McGraw-Hill Education; 2014

2. Jacobs. STP 8000 philosophy of the treatment process. Oyu Tolgoi Project; 2018. Document No.: CW2100430-S060-0001.

3. Mongolian Agency for Standardization and Metrology. Mongolian standards for water quality (MNS 0900:2018, MNS 6561:2024, MNS 4943:2015, MNS 4586:1998). Ulaanbaatar; 2024.

4. Fundamentals of Wastewater Treatment and Engineering
   Riffat R. Fundamentals of wastewater treatment and engineering. Boca Raton: CRC Press; 2012.

5. Principles of Membrane Bioreactors for Wastewater Treatment
   Park HD, Chang IS, Lee KJ. Principles of membrane bioreactors for wastewater treatment. Boca Raton: CRC Press; 2015.

6. Basic Environmental Technology
   Nathanson JA, Schneider RA. Basic environmental technology: water supply, waste management, and pollution control. 6th ed. Boston: Pearson; 2015.

7. Standard Methods for the Examination of Water and Wastewater
   American Public Health Association, American Water Works Association, Water Environment Federation. Standard methods for the examination of water and wastewater. 23rd ed. Washington (DC): APHA; 2017.

8. Ministry of Construction and Urban Development (Mongolia). Norms for drinking and domestic water consumption of populated areas BNbD 40-02-60. Ulaanbaatar; [year]. Table 5.1.1.

9. Ulaanbaatar Electricity Distribution Network (UBEDN). Electricity tariff [Internet]. Ulaanbaatar: UBEDN; [cited 2026 May 6]. Available from: https://tog.mn/une/1

Appendix A

MLSS and MLVSS Analysis Using Glass Fiber Filter (5mL Sample)

	Mass of filter (g)	Mass of filter after evaporation at 104°C (g)	Mass of filter after evaporation at 550°C (g)
Influent 1	0.097	0.100	0.098
Influent 2	0.098	0.100	0.099
Denitrification 1	0.097	0.144	0.107
Denitrification 2	0.097	0.147	0.108
Nitrification 1	0.098	0.135	0.106
Nitrification 2	0.098	0.135	0.106
MBR 1	0.097	0.133	0.106
MBR 2	0.097	0.133	0.107
Effluent 1	0.097	0.099	0.098
Effluent 2	0.097	0.099	0.098

$$MLSS = \frac{Mass\ of\ filter\ after\ evaporation\ at\ 100°C\ (g) - Mass\ of\ filter}{Sample\ volume\ (ml)} \times 1,000,000 \quad mg/l$$

$MLSS = \frac{0.100-0.097}{5} \times 1,000,000 = 600 \quad mg/l$ Influent 1

$MLSS = \frac{0.100-0.098}{5} \times 1,000,000 = 400 \quad mg/l$ Influent 2

$MLSS = \frac{0.144-0.097}{5} \times 1,000,000 = 9400 \quad mg/l$ Denitrification 1

$MLSS = \frac{0.147-0.097}{5} \times 1,000,000 = 10000 \quad mg/l$ Denitrification 2

$MLSS = \frac{0.135-0.097}{5} \times 1,000,000 = 7600 \quad mg/l$ Nitrification

$MLSS = \frac{0.133-0.097}{5} \times 1,000,000 = 7200 \quad mg/l$ MBR

$MLSS = \frac{0.099-0.097}{5} \times 1,000,000 = 400 \quad mg/l$ Effluent

Trial 2

	Mass of filter (g)	Mass of filter after evaporation at 104°C (g)	Mass of filter after evaporation at 550°C (g)
Influent 1 (after 2- 3 min settling)	0.1004	0.1028	0.1012
Influent 2	0.0988	0.1138	0.1091
Effluent 1	0.0989	0.1006	0.0995
Effluent 2	0.0986	0.0991	0.0983

$$MLSS_{influent} = \frac{0.1028-0.1004}{5} \times 1{,}000{,}000\ mg/l = 480\ mg/l$$
$$MLSS_{influent} = \frac{0.1138-0.1004}{5} \times 1{,}000{,}000\ mg/l = 2680\ mg/l$$
$$MLSS_{effluent} = \frac{0.1006-0.0989}{5} \times 1{,}000{,}000\ mg/l = 340\ mg/l$$
$$MLSS_{effluent} = \frac{0.0991-0.0986}{5} \times 1{,}000{,}000\ mg/l = 100\ mg/l$$

Trial 3

	Mass of filter (g)	Mass of filter after evaporation at 104°C (g)
Influent 1	0.1389	0.1503
Influent 2	0.1449	0.1596
Effluent 1	0.1419	0.1443
Effluent 2	0.1438	0.1465

$$MLSS_{influent} = \frac{0.1503-0.1389}{5} \times 1{,}000{,}000\ mg/l = 2280\ mg/l$$
$$MLSS_{influent} = \frac{0.1596-0.1449}{5} \times 1{,}000{,}000\ mg/l = 2940\ mg/l$$
$$MLSS_{effluent} = \frac{0.1443-0.1419}{5} \times 1{,}000{,}000\ mg/l = 480\ mg/l$$
$$MLSS_{effluent} = \frac{0.1465-0.1438}{5} \times 1{,}000{,}000\ mg/l = 540\ mg/l$$

Tank	Parameter	Replicate 1 (mg/L)	Replicate 2 (mg/L)	n	Mean (mg/L)	Std Dev s	Std Error SE	Min	Max	$t_{0.025}$ (df=n−1)	95% CI ($\bar{x} \pm t \cdot SE$)	RSE
Denitrification	MLSS (mg/L)	9400	10000	2	9700	424.3	300	9400	10000	12.706	9700.0 ± 3811.8	0.03
Nitrification	MLSS (mg/L)	7600	7600	2	7600	0	0	7600	7600	12.706	7600.0 ± 0.0	0.00
MBR	MLSS (mg/L)	7200	7200	2	7200	0	0	7200	7200	12.706	7200.0 ± 0.0	0.00
Denitrification	MLVSS (mg/L)	2000	2200	2	2100	141.4	100	2000	2200	12.706	2100.0 ± 1270.6	0.05
Nitrification	MLVSS (mg/L)	1600	1800	2	1700	141.4	100	1600	1800	12.706	1700.0 ± 1270.6	0.06
MBR	MLVSS (mg/L)	1800	2000	2	1900	141.4	100	1800	2000	12.706	1900.0 ± 1270.6	0.05

Appendix B

SRT Calculation

$$SRT = \frac{(414 \times 9700) + (729 \times 7600) + (82 \times 7200)}{38.7 \times 7600 + 1495 \times 14.17} = \frac{10{,}146{,}600}{431{,}220} = 32.18\ days$$

$$SRT_{denitrification} = \frac{VX}{Q_w \times X_w + Q_e \times X_e} = \frac{414 \times 9700}{25.70 \times 7600 + 1495 \times 14.17} = 12.73\ days$$

$$SRT_{nitrification} = \frac{VX}{Q_w \times X_w + Q_e \times X_e} = \frac{729 \times 7600}{25.70 \times 7600 + 1495 \times 14.17} = 17.57\ days$$

$$SRM_{mbr} = \frac{VX}{Q_w \times X_w + Q_e \times X_e} = \frac{82 \times 7200}{25.70 \times 7600 + 1495 \times 14.17} = 2\ days$$

Biological Kinetic Analysis

The kinetic performance of the system was evaluated using the Monod growth model and associated design equations. Standard kinetic coefficients for COD oxidation at 20°C were applied.

Influent COD (S_0) = 441.5 mg/L
Effluent COD (S) = 16.3 mg/L

Effluent Substrate Concentration (Theoretical)

The theoretical minimum effluent substrate concentration at steady state is determined from:

$$S = \frac{Ks(1 + k_d \times SRT)}{SRT \times (Y \times \mu max - k_d) - 1} = \frac{8.0 \times (1 + 0.12 \times 17.57)}{17.57 \times (0.45 \times 6.0 - 0.12) - 1} = 0.56\ mg/L$$

Biomass X

$$X = \frac{SRT \times Y \times (S_0 - S)}{\tau(1 + k_d \times SRT)}$$

$$X_{denitrification} = \frac{17.57 \times 0.45 \times (441.5 - 16.3)}{0.270\ (1 + 0.12 \times 12.73)} = 4926\ mg\ VSS/L$$

$$X_{nitrification} = \frac{17.57 \times 0.45 \times (441.5 - 16.3)}{0.476\ (1 + 0.12 \times 17.57)} = 2272\ mg\ VSS/L$$

$$X_{mbr} = \frac{17.57 \times 0.45 \times (441.5 - 16.3)}{0.053\ (1 + 0.12 \times 14.2)} = 23458\ mg\ VSS/L$$

Net Biomass Yield

The net (observed) biomass yield accounts for endogenous decay and is given by:

$$Y_{net} = \frac{Y}{1 + k_d \times SRT} = \frac{0.45}{3.108} = 0.144\ g\frac{VSS}{g}COD$$

This value indicates that for every gram of COD removed, approximately 0.166 g of volatile suspended solids (VSS) are produced on a net basis, which is significantly lower than the true yield (Y = 0.45 g VSS/g COD) due to endogenous respiration at the elevated SRT.

Specific Growth Rate

The specific growth rate of the biomass under operating conditions is described by the Monod equation:

$$\mu = \mu_{max}\frac{S}{K_S + S} = 6\ \times \frac{16.3}{8.0 + 16.3} = 4.03\ d^{-1}$$

The net specific growth rate, accounting for endogenous decay, is:

$$\mu_{net} = \mu - k_d = \ 4.03 - 0.12 = 3.91\ d^{-1}$$

Verification via 1/SRT Relationship

The consistency of the kinetic analysis was verified using the fundamental relationship between SRT and substrate utilisation rate U:

$$\frac{1}{SRT} = Y \times U - K_d$$

where U is the specific substrate utilisation rate (d^{-1}):

$$U = \frac{S_0 - S}{\tau \cdot X} = \frac{425.2}{0.476 \times 2272} = 0.393\ d^{-1}$$

$$\frac{1}{SRT} = Y \times U - K_d = 0.45 \times 0.393 - 0.12 = 0.057$$

$$SRT = \frac{1}{0.057} = 17.5\ days$$

The calculated SRT of 14.3 days is consistent with the operationally determined nitrification SRT of 14.2 days, confirming the internal consistency of the kinetic model.

Temperature Correction to 12°C (Winter Scenario)

Effluent Substrate (S)

$$S = \frac{Ks(1 + k_d \times SRT)}{SRT \times (Y \times\ \mu max - k_d) - 1} = \frac{5.846 \times (1 + 0.12 \times 17.57)}{17.57 \times (0.45 \times 3.492 - 0.12) - 1} = 0.74\ mg/L$$

$$\mu = \mu_{max}\frac{S}{K_S + S} = 3.492 \times \frac{16.3}{5.846 + 16.3} = 2.571\ d^{-1}$$
$$\mu_{net} = \mu - k_d = 2.571 - 0.12 = 2.451\ d^{-1}$$

For NH4 (20°C)

$$S_0 = 76.06$$
$$S = 1.18$$

ΔS = 74.88 mg/L

$$SRT_{min,nitrification} = \frac{1}{\mu max - k_d} = \frac{1}{0.9 - 0.17} = \frac{1}{0.73} = 1.37\ days$$

1. Substrate

$$S = \frac{Ks\left(\frac{1}{SRT} + k_d\right)}{\mu max - k_d - \frac{1}{SRT}} = \frac{0.5\left(\frac{1}{17.57} + 0.17\right)}{0.9 - 0.17 - \frac{1}{17.57}} = 0.169\ mg\ NH_4/L$$

2. Biomass X

$$X = \frac{SRT \times Y \times (S_0 - S)}{\tau(1 + k_d \times SRT)}$$

$$X_{nitrification} = \frac{17.57 \times 0.15 \times (74.88)}{0.476\ (1 + 0.17 \times 17.57)} = 104\ mg\ VSS/L$$

3. Net biomass yield

$$Y_{net} = \frac{Y}{1 + k_d \times SRT} = \frac{0.15}{1 + 0.17 \times 17.57} = 0.0376\ g\frac{VSS}{g}COD$$

4. μ — Specific Growth Rate:

$$\mu = \mu_{max}\frac{S}{K_S + S} = 0.9 \times \frac{1.18}{0.5 + 1.18} = 0.632\ d^{-1}$$

5. Net Growth Rate:

$$\mu_{net} = \mu - k_d = 0.632 - 0.17 = 0.462\ d^{-1}$$

Verification via 1/SRT Relationship

$$U = \frac{S_0 - S}{\tau \cdot X} = \frac{74.88}{0.476 \times 104} = 1.51\ d^{-1}$$
$$\frac{1}{SRT} = Y \times U - K_d = 0.15 \times 1.51 - 0.17 = 0.0565$$
$$SRT = \frac{1}{0.0565} = 17.5\ days$$

Temperature Correction to 12°C

$$SRT_{min,nitrification} = \frac{1}{\mu max - k_d} = \frac{1}{0.516 - 0.17} = \frac{1}{0.346} = 2.89\ days$$
$$S = \frac{Ks\left(\frac{1}{SRT} + k_d\right)}{\mu max - k_d - \frac{1}{SRT}} = \frac{0.393\left(\frac{1}{17.57} + 0.17\right)}{0.516 - 0.17 - \frac{1}{17.57}} = 0.308\ mg\ NH_4/L$$
$$\mu = \mu_{max}\frac{S}{K_S + S} = 0.516 \times \frac{1.18}{0.393 + 1.18} = 0.387\ d^{-1}$$

$$\mu_{net} = \mu - k_d = \ 0.387 - 0.17 = 0.217\ d^{-1}$$

Appendix C

Biomass Mass balance

To verify the internal consistency of the system and determine the recirculation sludge concentration entering the denitrification zone, a biomass mass balance was performed across the treatment system using Equation (2.22):

$$Q_{in}\ \times X_{in} + Q_r\ \times X_r = Q_{eff}\ \times X_{eff} + Q_w\ \times X_w$$

Substituting the known values:

$$\frac{1421 \times 500}{1000} + \frac{1920 \times 7200}{1000} = \frac{1497.17 \times 400}{1000} + \frac{38.7 \times 7400}{1000}$$

$$14534.5 = 885.25\ +\ Q_r\ \times X_r\ (residual\ term)$$

Since the left-hand side (14,534.5 kg/d) does not balance with the right-hand side outputs alone (885.25 kg/d), this confirms the presence of a significant internal recirculation solids load returning to the denitrification zone. Rearranging the mass balance to solve for the recirculation sludge concentration X_r entering the denitrification tank:

$$X_r = \frac{14534.5 - 885.25}{1920} \times 1000 = 7110\ \text{mg/L}$$

This result indicates that approximately 7,110 mg/L of mixed liquor suspended solids are recirculated from the MBR tank back to the denitrification zone. The recirculation flow rate of *Q*r = 1,920 m³/d was estimated based on an average return flow of 80 m³/h operating continuously over 24 hours.

Exponential growth equation

Starting from the current condition where Qw is approximately 20 m³/day, a daily 2% stepwise increase in wasting flow is recommended. Based on exponential growth calculation, reaching a Qw of 70 m³/day from 20 m³/day at 2% daily increment requires approximately 63 days: $Q_t = Q_0 \times (1.02)^t$

$$t = \frac{ln(70/20)}{ln(1.02)} = \frac{ln(3.5)}{0.0198} = 64\ days$$

Table 22. Proposed Daily Sludge Wasting Flow Rate (Qw) Based on 2% Stepwise Increase

Day	Qw (m^3/day)	Day	Qw (m^3/day)
1	20.00	41	44.16
2	20.40	42	45.04
3	20.81	43	45.94
4	21.22	44	46.86
5	21.65	45	47.80
6	22.08	46	48.76
7	22.52	47	49.73
8	22.97	48	50.73
9	23.43	49	51.74
10	23.90	50	52.78
11	24.38	51	53.83
12	24.87	52	54.91
13	25.36	53	56.01
14	25.87	54	57.13
15	26.39	55	58.27
16	26.92	56	59.43
17	27.46	57	60.62
18	28.00	58	61.84
19	28.56	59	63.07
20	29.14	60	64.33
21	29.72	61	65.62
22	30.31	62	66.93
23	30.92	63	68.27
24	31.54	64	69.64
25	32.17	65	71.03
26	32.81		
27	33.47		
28	34.14		
29	34.82		
30	35.52		
31	36.23		
32	36.95		
33	37.69		
34	38.44		
35	39.21		
36	40.00		
37	40.80		
38	41.61		
39	42.45		
40	43.29		